

Chapter 17  
 AERIALS  
 List of Contents

	Sect.
Fundamental considerations	1
<b>Transmitting aerials</b>	
Type of wave emitted by a transmitting aerial	2
Field-strength diagram of an aerial	3
Field strength diagram of half-wave aerial	4
Isotropic radiator	5
Energy density in an electromagnetic wave	6
Power relations for a plane electromagnetic wave	7
Power and field relations for an isotropic radiator	8
Power and field relations for any aerial	9
Power gain of half-wave aerial	10
Input impedance	11
Q-factor of a resonant-length aerial	12
Factors affecting the resonant length	13
<b>Receiving aerials</b>	
General	14
Power relations for an isotropic receiving aerial	15
Power relations for any receiving aerial	16
Transmission and reception	17
<b>Propagation and reception of short waves</b>	
Scattering by an obstacle	18
Range of a radar set	19
Reflection from ground and sea	20
Horizontally polarised waves incident on ground	21
Horizontally polarised waves incident on sea	22
Reflection of vertically polarised waves	23
Effect of flat earth on field strength diagram (Horizontal polarisation)	24
Effect of flat earth on field strength diagram (Vertical polarisation)	25
Summary of effect of flat surface	26
Gap filling	27
Effect of earth's curvature : refraction	28
<b>Common types of aerial arrays</b>	
Broadside array	29
Linear broadside array	30
Complete broadside array	31
Use of reflecting screen behind broadside array	32
Wire netting reflector screens	33
Power gain of broadside array	34
Feeding arrangements for broadside arrays	35
Example of a complete broadside array	36
Tapered feed to linear broadside arrays	37
Beam swinging with linear broadside arrays	38
End-fire arrays	39
Comparison of end-fire and broadside arrays	40
Parasitic director	41
End-fire array with parasitic directors (Yagi)	42
Parasitic reflector	43
Use of folded half-wave aerial	44

	Sect.
Bandwidth of arrays	45
Effect of ground on aerial arrays	46
Gap-filling by means of phasing	47
Microwave aeriels	
Paraboloidal mirrors	48
Primary feeds for paraboloidal mirrors	49
Beam swinging with paraboloidal mirrors	50
Specially shaped mirrors	51
Cheese type of mirror	52
Band-width of mirror-type aeriels	53
Slots in waveguides	54
Slotted linear arrays	55
Slotted waveguide with mirror	56
Microwave beacon aeriels	57
Effect of ground on microwave aeriels	58
Conclusion	59

## CHAPTER 17

### AERIALS

#### 1. FUNDAMENTAL CONSIDERATIONS

The direction-finding methods adopted in radar rely almost entirely on the use of an aerial system with known directional properties. Consequently, one is concerned here, much more than in communications, with the theory and design of aerial systems with specified directional performance. Again, in radar one is nearly always working with relatively weak received signals. Consequently, in the design of a radar set to give a specified range of detection, one requires to know the efficiency of the aerials in producing an electromagnetic field at the echoing object and in collecting or receiving back the small return signal or Echo. This aspect of aerials is referred to as the gain. The directional performance and gain are obviously closely connected; a highly beamed system will have a large gain. Finally, as in communications, one is often concerned with the impedance which the aerial presents to the transmission line connecting it with the transmitter or receiver. Often, for example, one requires an aerial whose impedance does not vary very much with change of frequency.

There are, therefore, three points in which one is usually interested when discussing an aerial: its directional properties, gain and input impedance.

A quantitative discussion of the working of the RF side of a radar system is best done from the point of view of power relationships. One is not so much concerned therefore with the number of amperes flowing in the transmitting aerial as with the number of watts it is radiating. Indeed, the form of the aerials (mirror, horn, waveguide, etc) usually makes it difficult to decide the point where an "aerial ammeter" might be connected. Also with receiving aerials one is not usually concerned with the "effective height" or received field strength or voltage, but rather with the "effective area" relating to the amount of power which the receiving aerial intercepts from the incident wave. Hence in what follows considerable emphasis will be laid on power relationships, and a minimum of discussion will be given on the flow of RF current in the aerials.

#### TRANSMITTING AERIALS

##### 2. Type of Wave Emitted by a Transmitting Aerial

The radiated electromagnetic field, when observed in free space at a large distance from any aerial, is similar to the plane wave discussed in Chap. 5 Sec. 2. There is a transverse electric field  $\vec{E}$  and also a transverse magnetic field  $\vec{H}$  which lie in the wave-front, at right angles to one another and oscillating in phase. The wave-front travels out with velocity  $c$ , where

$$c = 3 \times 10^8 \text{ metres/second} \dots\dots\dots (1)$$

The wavelength  $\lambda$  is related to the frequency  $f$  of the transmitter by the relation

$$c = \lambda f \dots\dots\dots (2)$$

The wave-front is, however, only approximately plane. In fact it is spherical, with the aerial at the centre of the sphere. At large distances a portion of the sphere can be regarded as plane, but due to this spherical spreading the field becomes weaker as the distance  $r$  from the aerial increases.

This spherical spreading of energy is common to many branches of physics. The intensity depends on the surface area, the product of intensity and area remaining constant. For a sphere the surface area is proportional to  $r^2$ . Thus the law for such phenomena is termed the Inverse Square Law. Hence the power  $P$  in an electromagnetic wave is given by :-

$$P \propto \frac{1}{r^2} \dots\dots\dots (3)$$

However, the electric field  $E$  is proportional to  $\sqrt{P}$  (see Sec. 7). Thus the electric field strength  $E$  follows the law :-

$$E \propto \frac{1}{r} \dots\dots\dots (4)$$

In what follows the electric field in a wave will usually be considered, but it must be remembered that the magnetic field also is necessarily present.

3. Field-Strength Diagram of an Aerial

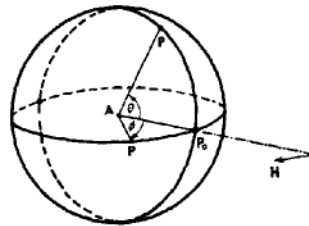


Fig.741. - Method of taking field strength diagrams.

In Sec. 2 the variation of field with distance was discussed, leading to equation (4). This formula applies when one travels out from the aerial in a fixed direction. It is desired now to consider how  $E$  varies when the point of observation is maintained at a fixed distance from the aerial but moves so that the line from the aerial to the observer varies in direction. This means that the point of observation  $P$  must be moved over a large sphere of radius  $r$  with the aerial  $A$  as centre (Fig.741). The value of  $E$  is required at all points on the sphere. In practice one often simplifies this by taking two perpendicular great circles, as shown in Fig.741, and observing first round one circle ( $\theta$  variation) and then round the other ( $\phi$  variation).

As remarked in Sec. 2, the radiated wave consists of  $\vec{E}$  and  $\vec{H}$  at right angles. They determine the Polarisation of the wave, e.g., horizontal polarisation if  $\vec{E}$  is horizontal and vertical polarisation if  $\vec{E}$  is vertical. We can therefore choose the planes of one of the great circles in Fig.741 (say the plane of  $\theta$ -variation) to be parallel to the direction of  $\vec{E}$  and the other (plane of  $\phi$ -variation) to be parallel to the direction of  $\vec{H}$ . The field strength diagrams are then said to be in the  $E$ -plane and  $H$  plane respectively.

There is nearly always one particular position  $P_0$  on the sphere where the field strength is a maximum, since most aeri- als introduce a certain amount of beaming. It is convenient to make  $AP_0$  (Fig.741) the line of intersection of the great circles and to measure the angles  $\theta$  and  $\phi$  from this direction.

If the field at  $P_0$  is  $E_0$ , then  $E$  at any other point  $P$  on the sphere will be expressible in the form

$$E = E_0 f(\theta, \phi) \dots\dots\dots (5)$$

$f(\theta, \phi)$  is the ratio of the electric field at any point  $(\theta, \phi)$  compared with the electric field in the direction of maximum field strength. The solid figure defined by  $r = f(\theta, \phi)$  is termed the three-dimensional polar diagram. In the planes  $\phi = 0, \theta = 0, r = f(\theta, \phi)$  gives two-dimensional polar diagrams in the E and H planes respectively. These are easily shown graphically and are indicative of the three-dimensional figure.

4. Field-Strength Diagram of Half-Wave Aerial

The half-wave aerial consists of a wire half a wavelength long with a gap at the centre to which a balanced feeder is attached (Fig.742) leading from a transmitter. The current set up in the wire is not of uniform amplitude, being zero at the ends and a maximum in the middle. By analogy with standing waves on transmission lines or lecher bars, the current distribution expected is sinusoidal. However, owing to feeding and end-effects the distribution is only approximately sinusoidal in amplitude and the phase is not uniform. The exact results lead to difficult mathematical manipulation and the sine-wave amplitude distribution and uniform phase give results which are comparable with those obtained in practice. It will be assumed then, that the current has the same phase all along the aerial, the currents at all points on the wire rising and falling together but to different amplitudes. This is illustrated in Fig.743. The current in the wire arises from the movement of electric charges (e.g. electrons). In any small part of the wire, such as the point P in Fig.743, the charges are first moving upwards then they are slowed down to rest. Next they are moving downwards and then brought to rest again. Consider a charge moving upwards with uniform speed (Fig.744); lines of electric force will run out from this charge in all directions. Wherever the electric field is changing it is accompanied by a magnetic field the strength of which is proportional to the rate of change of the electric field. Now let the charge be brought to rest, i.e., decelerated. The electric lines will tend to go on but will be pulled back by the charge. "Kinks" will develop in the lines of force and will travel outwards, straightening out the lines of force to their correct positions relative to the charge (Fig.745). We may regard the lines of force as being in tension, with the tension greater in the kink than in the line itself. The kink is the seat of an intense field and is travelling outwards to form the electromagnetic wave radiated by the charge as its velocity is reduced to zero. The radial electric field is weak and negligible at large distances, but the kink is strong. The strongest stretching occurs in the kink of a line such as CD (Fig. 745) at right angles to AB, the direction of deceleration. In any other direction CF, making an angle  $\theta$  with CD,

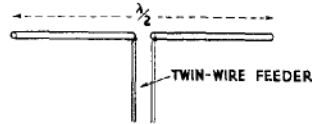


Fig.742.- Half-wave centred-fed aerial.

This is illustrated in Fig.743. The current in the wire arises from the movement of electric charges (e.g. electrons). In any small part of the wire, such as the point P in Fig.743, the charges are first moving upwards then they are slowed down to rest. Next they are moving downwards and then brought to rest again. Consider a charge moving upwards with uniform speed (Fig.744); lines of electric force will run out from this charge in all directions. Wherever the electric field is changing it is accompanied by a magnetic field the strength of which is proportional to the rate of change of the electric field. Now let the charge be brought to rest, i.e., decelerated. The electric lines will tend to go on but will be pulled back by the charge. "Kinks" will develop in the lines of force and will travel outwards, straightening out the lines of force to their correct positions relative to the charge (Fig.745). We may regard the lines of force as being in tension, with the tension greater in the kink than in the line itself. The kink is the seat of an intense field and is travelling outwards to form the electromagnetic wave radiated by the charge as its velocity is reduced to zero. The radial electric field is weak and negligible at large distances, but the kink is strong. The strongest stretching occurs in the kink of a line such as CD (Fig. 745) at right angles to AB, the direction of deceleration. In any other direction CF, making an angle  $\theta$  with CD,

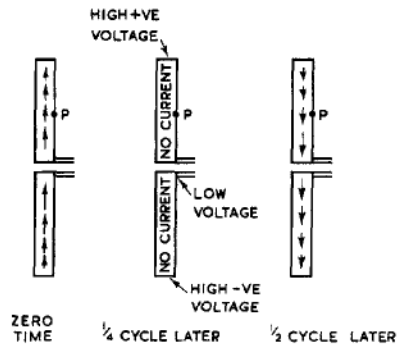


Fig.743.- Current and voltage on half-wave aerial.



Fig. 744. - Electric field around charge moving with uniform speed.

the kink is less pronounced. It is the component of the kink at right angles to the electric line which constitutes the radiated field. The radiated field is therefore proportional to  $\cos \theta$ , this being the component of the deceleration of the charge at right angles to the electric line CF. Note that when the movement of the charge is sinusoidal instead of in jerks as hitherto considered the field is a maximum when the charge is at rest, i.e., when the current is zero. Thus the radiated field lags  $90^\circ$  on the current.

The charges all along the wire are radiating and the field is obtained by adding up the wavelets sent out by each accelerated (or decelerated) charge. Thus the following results may be deduced (Fig. 746) :-

- (i) Since the polarisation of the wave radiated from each charge is such that E always lies in a plane through the aerial, (see Fig.746) the same condition holds for the resultant wave radiated from the whole of the half-wave dipole.
- (ii) Since the dipole has axial symmetry, the field-strength diagram is symmetrical about a line drawn through the axis of the dipole; in other words, the H-plane field-strength diagram is given by

$$E = E_0 \dots\dots\dots (6)$$

In polar co-ordinates this equation represents a circle.

- (iii) The radiated field strength for each individual charge is proportional to  $\cos \theta$ , so that

$$E = E_0 \cos \theta \dots\dots\dots (7)$$

A similar result holds for the dipole as a whole. This result would be identical with (7) if we could assume that the wavelets from different charges along the aerial add together arithmetically. In fact, this is not exactly true. The wavelets from  $P_1, P_2$  in Fig.747 do not arrive at a distant point P quite at the same time as a wavelet from the centre C of the wire. The wavelet from  $P_1$  arrives earlier due to the path difference CD and that from  $P_2$  arrives the same amount later due to the path difference  $P_2F$ . When we add together the effects from  $P_1$  and  $P_2$  we must therefore make a vector addition so as to

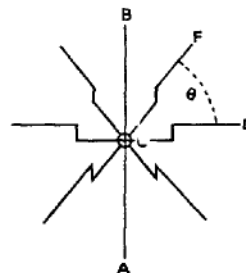


Fig.745.- Kinks in electric lines due to a deceleration of moving charge.

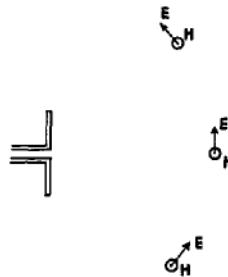


Fig.746.- Polarisation of wave from half wave aerial - E in plane of paper and H perpendicular to plane of paper.

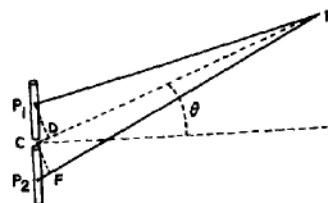


Fig. 747.- Phase difference between rays from pairs of points on half-wave aerial.

allow for the phase lead and lag (Fig.748). The resultant has the same phase as the wavelet from the mid-point of the aerial so that we may say, first of all, that the field appears to come from the mid-point C of the aerial. This point is called the Phase Centre. Next we note

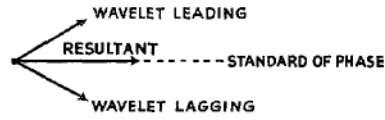


Fig.748.- Addition of wavelets.

that the phase lead or lag is greater as we move P<sub>1</sub> and P<sub>2</sub> out to the ends of the aerial. Failure to use the vector method of addition is therefore more serious for wavelets from near the ends of the aerial than for wavelets near the centre. The latter are, however, more important than the former since the current is strongest near the centre. The phase difference between wavelets gets larger as one moves round from  $\theta = 0$  to  $\theta = 90^\circ$ . The wave is therefore rather less intense away from the  $\theta = 0$  position than one would find simply by arithmetical addition of wavelets.

If the effects due to each elemental length are integrated over the length of the aerial the resultant field-strength diagram for a  $\lambda/2$  aerial is given by :-

$$E = E_0 \frac{\cos \left[ \frac{\pi}{2} \sin \theta \right]}{\cos \theta} \dots \dots \dots (8)$$

It is convenient to denote the E-plane Field-Strength Factor of a  $\lambda/2$  aerial by a symbol, say D,

$$\text{where } D = \frac{E/E_0}{\cos \theta} = \frac{\cos \left( \frac{\pi}{2} \sin \theta \right)}{\cos \theta} \dots \dots \dots (9)$$

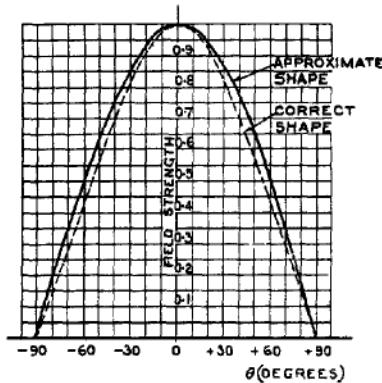


Fig.749.- Field strength diagram of half-wave aerial.

A plot of equation (7) is shown in Fig.749 with the curve corresponding to the correct equation (8) indicated dotted. It will be seen that the difference between the results for equations (7) and (8) is small. It is frequently convenient for mathematical derivations to assume that  $D = \cos \theta$ , the order of error being indicated. A plot in polar coordinates is often used, the radius from an origin O being taken to represent E at the appropriate angle. This method of plotting is shown in Figs.750 and 751 for equations (8) and (6) respectively. The field at a distance r measured out in any direction, not necessarily in the E - or H - plane, is similarly indicated by drawing radii of lengths proportional to E. The ends of these radii lie on a surface as shown in Fig.752.



Fig.750.- Field-strength diagram of half-wave aerial (E-plane); aerial in plane of paper.



Fig.751.- Field-strength diagram of half-wave aerial (H-plane); aerial at right angles to plane of paper.

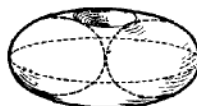


Fig.752.- Field-strength diagram of half-wave aerial (all directions).

5. Isotropic Radiator

Although the half-wave aerial is the simplest met with in practice, its field-strength diagram as shown in Fig.752 is still rather complicated and as a standard of reference it is convenient to consider a hypothetical aerial which radiates equally in all directions. Its field-strength diagram plotted in polar co-ordinates is a sphere. This aerial is sometimes called an Isotropic Radiator.

6. Energy Density in an Electromagnetic Wave

The electromagnetic wave propagated from an aerial is continually carrying away energy, which must be supplied by the transmitter. Recalling again that the wave consists of an electric field and a magnetic field, we see that energy is divided into two parts, electric energy carried by the electric lines of force and magnetic energy carried by the magnetic lines. These two energies are equally important and are in fact equal in magnitude in a plane wave. Electric energy by itself is familiar from consideration of a condenser charged up to a steady potential. Consider the condenser to be made of two plates each being one metre square, and placed one metre apart, with air dielectric; (Fig.753).

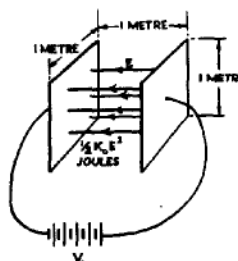


Fig.753.- Electric field energy.

Its capacity  $K_0$  is readily calculable to be

$$K_0 = \frac{10^{-9}}{36\pi} \text{ farads} \dots\dots\dots (10)$$

The energy,  $W$  (electric) stored in the condenser when there is a potential difference of  $V$  volts across the plates is given by the formula

$$W(\text{electric}) = \frac{1}{2} K_0 V^2 \text{ joules} \dots\dots\dots (11)$$

Regarding the electric field  $E$  in the space between the plates as the seat of this energy we may rewrite (11) as follows :-

Since the distance between the plates is 1 metre, a potential difference  $V$  volts means a field  $E$  volts/metre where

$$E = V \dots\dots\dots (12)$$

Also the volume of the space between the plates is 1 cubic metre. Hence (11) becomes :-

$$W_v (\text{electric}) = \frac{1}{2} K_0 E^2 \text{ joules/cubic metre} \dots\dots\dots (13)$$

and we can apply (13) to give the energy density of any steady electric field in air. Now in the wave, one is dealing with an alternating electric field. The same formula (13) will apply, however, provided E is taken to be the RMS value of the field strength. It has already been remarked that in a plane electromagnetic wave in space the magnetic energy is equal to the electrical energy. Thus the total energy density  $W_v$  for a wave whose electric field is E RMS volts per metre will be twice expression (13); i.e.,

$$W_v = K_0 E^2 = \frac{10^{-9} E^2}{36\pi} \text{ joules/cubic metre ..... (14)}$$

7. Power Relations for a Plane Electromagnetic Wave

Consider a wave of cross-sectional area one square metre (Fig. 754). Let an observer O stand near A watching the cross-section there. The wave is supposed to be moving to the right with velocity c metres/second given by equation (1). Now measure back from A a distance AB where

AB = c metres .....(15)

The energy density  $W_v$  of the wave is given by (14). Hence the energy in the portion AB is

$c \cdot 1 \cdot 1 \cdot W_v$  joules;

i.e., using (1) and (14) the energy is

$$\frac{3 \times 10^8 \times 10^{-9} \times E^2}{36\pi} \text{ joules}$$

or, simplifying,

$$E^2/120\pi \text{ joules ..... (16)}$$

In one second the section BA will have moved to the right so that B is opposite the observer O, since B moves with speed c metres/second. Thus the energy that has passed through the cross-section at O in one second is that contained in the portion AB. This, with (16), leads to the important expression for the power  $P_a$  passing through a square metre of wavefront :-

$$P_a = E^2/120\pi \text{ joules/sec/metre}^2 = E^2/120\pi \text{ watts/metre}^2 \text{ ..... (17)}$$

This equation is quite analogous to the formula for the power P dissipated in a resistance R ohms with an RMS voltage V across it :-

$$P = V^2/R \text{ watts ..... (18)}$$

From a comparison of (17) with (18) it follows that the factor 120π in (17) must have the dimensions of ohms. This number is therefore sometimes called the wave impedance, denoted by  $Z_w$ . We thus have

$$Z_w = 120\pi = 377 \text{ ohms ..... (19)}$$

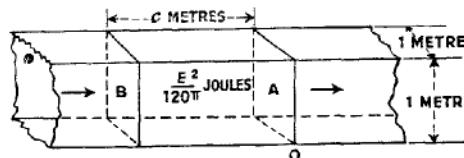


Fig.754.- Power carried by a wave

and

$$P_a = E^2/Z_w \dots\dots\dots (20)$$

The relations of this and the preceding paragraph apply to waves in air or free space. If the dielectric constant K and permeability  $\mu$  of the medium are not unity the expressions have to be modified slightly by the introduction of K and  $\mu$  into the equations.

8. Power and Field Relations for an Isotropic Radiator

The power from an isotropic radiator flows out equally in all directions. Thus if the transmitter puts P watts into the aerial it is possible to calculate the power passing through a square metre of wavefront at any distance. Suppose it is required to find the effect at distance r metres from the aerial. Draw a sphere of radius r metres, with the aerial as centre. The area A of the surface of the sphere is

$$A = 4 \pi r^2 \dots\dots\dots (21)$$

The power P is passing out uniformly through this area. Hence  $P_a$ , the power per unit area of wavefront at distance r from this aerial, is given by

$$P_a = P/4 \pi r^2 \text{ watts/ square metre} \dots\dots\dots (22)$$

Equations (17) and (22) enable the RMS field strength E to be expressed in terms of the input power P and the distance r. We have

$$\frac{E^2}{120\pi} = \frac{P}{4\pi r^2}$$

or

$$E = \frac{\sqrt{30P}}{r} \text{ RMS volts/metre} \dots\dots\dots (23)$$

for an isotropic radiator.

9. Power and Field Relations for Any Aerial

Even the simplest aerial, the half-wave aerial, does not transmit power equally in all directions, and in general, as remarked in Sec. 3, there is a "best" direction into which most power is sent. Suppose a given aerial is required to produce a field strength  $E_0$  at a point distant r. The aerial is disposed so that the distant point lies in the aerial's best direction. It is then supplied with power P. This power will be less than the power, P' say, required by an isotropic radiator to give the same field at a distance r. The given aerial is thus more economical to use than the isotropic radiator and is said to have a Power Gain g where

$$g = P'/P \dots\dots\dots (24)$$

(As mentioned in Chap. 3 Sec.5, gain is usually expressed as the logarithm of a ratio, whereas here it is simply the ratio.) The power gain of an aerial can be measured experimentally or, in a few cases, it may be calculated. If the power gain is known, then the performance of the aerial in its best direction is equal to that of an isotropic radiator, supplied with g times the power. Hence the field strength at distance r from an aerial supplied with power P is given by (23) after replacing P by gP, i.e.,

$$E_0 = \frac{\sqrt{30Pg}}{r} \text{ RMS volts/metre} \dots\dots\dots (25)$$

for an aerial of gain  $g$ , in its best direction.

Example

A highly beamed aerial used in a radar set has a power gain of 300. The power output is 100 kilowatts. What field strength would be detected by an enemy listening station 50 kilometres away ?

(a) From equation (25) we have

$$E_0 = \sqrt{\frac{30,100,000 \cdot 300}{50,000}}$$

$$= 0.6 \text{ RMS volts/metre,}$$

(b) The answer may also be obtained from first principles, using the result that power per square metre is  $E^2/120\pi$

Thus :-

Suppose that an isotropic radiator is fed with 100 kilowatts. Consider a sphere of radius 50,000 metres. The area of the surface of this sphere is

$$4\pi \cdot 25 \cdot 10^8 \text{ square metres.}$$

Hence the power per square metre at the surface of this sphere is

$$\frac{10^5}{4\pi \cdot 25 \cdot 10^8} \\ = 10^{-5}/\pi \text{ watts/square metre}$$

With a gain of 300 we should obtain

$$\frac{300 \times 10^{-5}}{\pi} \text{ watts/square metre.}$$

Hence required field strength  $E_0$  is given by

$$\frac{E_0^2}{120\pi} = \frac{300 \times 10^{-5}}{\pi};$$

$$\text{i.e., } E_0^2 = 0.36$$

$$\text{or } E_0 = 0.6 \text{ RMS volts/metre.}$$

10. Power Gain of Half-Wave Aerial

The field-strength diagram of a half-wave aerial gives the variation of field strength  $E$  at a given distance  $r$  as the direction of the observation point is varied. Knowing the field-strength diagram of any aerial one can, in theory at least, deduce the gain in the following manner. Draw a sphere of radius  $r$  with the aerial at the centre and divide the surface up into small areas such as  $dA$ . Find from the field-strength diagram the field strength  $E$  at any small area on the sphere. The power flowing through the area is proportional to  $E^2 \cdot dA$  and so a measure of the power coming from the transmitter is obtained by integrating  $E^2 \cdot dA$  over the surface of the sphere. Now obtain from the field-

strength diagram the field strength  $E_0$  in the best direction (and using the same units as before). From an isotropic radiator one would obtain  $E_0$  all over the sphere's surface and the power required to maintain this would be proportional to  $4\pi r^2 E_0^2$ . The ratio of this to the power required by the given aerial gives the power gain. For the half-wave aerial we have approximately

$$E = E_0 \cos \theta$$

where  $E_0$  can be taken as unity. Thus the power required is proportional to

$$\iint \cos^2 \theta \, dA$$

the integration being over a sphere of radius  $r$ . This gives  $\frac{8\pi r^2}{3}$  and,

dividing into  $4\pi r^2$ , we obtain the result that the gain of a half-wave aerial is  $3/2(1.8 \text{ db.})$  The gain is in fact a little greater than 1.5 since the field-strength is rather sharper than  $\cos \theta$ . An integration using the exact formula gives the correct result as 1.6 (or 2.04db).

In general, for any aerial, we may write

$$E \propto f(\theta, \phi) \dots\dots\dots (26)$$

where  $f(\theta, \phi) = 1$  in the best direction. Then

$$g = \frac{4\pi r^2}{\iint f^2(\theta, \phi) \, dA} \dots\dots\dots (27)$$

the integration being over a sphere of radius  $r$ . Equation (27) can also be written

$$g = \frac{4\pi}{\iint f^2(\theta, \phi) \, d\omega} \dots\dots\dots (28)$$

where  $d\omega$  is the element of the solid angle =  $dA/r^2$ .

11. Input Impedance

Since the radiated wave carries power away from the transmitter an aerial can often be simulated by an impedance  $R_r + jX_r$ . The resistive part  $R_r$  of the dummy aerial must dissipate as heat the same amount of power as the aerial radiates. It is usually called the Radiation Resistance. The reactive part  $X_r$  corresponds to the storage of field energy in the vicinity of the aerial in the same way as energy is stored in a condenser or coil. Such stored energy near the aerial does not travel out into space like the radiated energy. Unlike the energy in a plane wave propagated out into space, the energy in the reactive storage field is not necessarily equally divided into electric energy and magnetic energy, and the aerial reactance may be capacitive or inductive according to which type of stored energy predominates. By special design, however, the two may be made equal and then the reactive term becomes zero. An aerial which is designed so that it has no reactive component of input impedance is termed a resonant aerial. The factors determining the resonant length are discussed later (Sec. 13). The shortest resonant length for a centre-fed aerial is just less than  $\lambda/2$ . It is usual to talk of a  $\lambda/2$  aerial when the resonant length aerial is meant. The value of the radiation resistance is calculated from the current at the terminals and the power radiated. This involves a fairly detailed investigation and the result for the centre-fed half-wave aerial in free space is 73 ohms.

Fig.743 shows that the centre-fed half-wave aerial is being driven at a place where the current is high and voltage low, and the radiation resistance would be expected to be comparatively low. This type of aerial is said to be Current-Fed. If, however the feeder is attached to the end of the aerial as in Fig.755 it is fed at a place where the voltage is high and the current low. This method of End-Feeding is therefore referred to as Voltage-Feed. The input resistance for a voltage-fed half-wave aerial is very high, its exact value depending on the thickness of the aerial wire or tube. A voltage-fed half-wave aerial shown connected as in Fig.755 unbalances the feeder. Voltage-fed aerials are therefore often used in pairs, one on each side of the feeder, as shown in Fig.756. The pair is sometimes referred to as a Full-Wave Aerial or better, as an End-Fed Pair. The radiation resistance of such a pair of voltage-fed (or end-fed) half-wave aerials is given in the following table. These results have been verified by experiment.

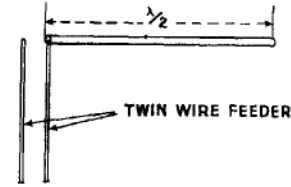


Fig.755.- Voltage feed to half-wave aerial.

Radiation Resistance of a Pair of Voltage-Fed Half-Wave Aerials made of Cylindrical Tubing

(Fig.756)

Wavelength/diameter	Resistance in ohms
100	920
200	1300
300	1500
400	1700
600	2000
800	2200
1000	2400
2000	3000
3000	3300
4000	3600
6000	4000
8000	4300
10000	4600

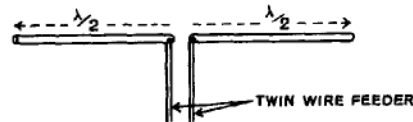


Fig.756 - Pair of half-wave aerials voltage fed (end-fed pair).

The field-strength diagram and power gain of the pair is different from that of a single half-wave aerial and is discussed in Sec. 30.

12. Q-Factor of a Resonant-Length Aerial

Only when it is cut to resonant length, i.e., a little less than  $\lambda/2$ , is the input impedance of a centre-fed aerial equal to a resistance of 73 ohms without reactance. When it is longer than the resonant length the impedance is inductive and when shorter it is capacitive. This may be deduced by comparing the half-wave aerial with a short section of open-circuited transmission line approximately  $\frac{\lambda}{4}$  in length (Chap. 4 Sec. 14).

Thus if the aerial is cut to be a resonant length for a certain transmitter frequency  $f_0$  and then the frequency is raised higher than  $f_0$  the aerial becomes inductive, and if lower it becomes capacitive. The aerial thus behaves like a series tuned circuit, consisting as in Fig.757 of a coil L, condenser C and resistance 73 ohms.

The values of L and C are such that at frequency  $f_0$  their reactances are equal and opposite so that they cancel out and the circuit appears like a resistance of 73 ohms. The input impedance (magnitude and phase) of the resonant length aerial is therefore of the form shown in Fig.758. One is usually interested in the selectivity or sharpness of the impedance curve, i.e., the Q-factor of the aerial.

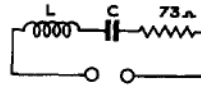


Fig.757.- Equivalent circuit of centre-fed half-wave aerial.

It is found that this depends on the thickness of the tubing or wire from which the aerial is made. Thin aerials have a higher Q than thick ones. The Q-factor of a resonant length aerial is given in the following table. This is based on theory, the results applying to either centre-fed or end-fed aerials. Few figures are available on the practical side but the values of Q obtained experimentally appear to be rather higher than the theoretical ones.

Theoretical Q-Factor of a Resonant length Aerial made of Cylindrical Tubing

Wavelength/diameter	Q
10	1.6
25	2.7
50	3.5
100	4.3
200	5.2
300	5.7
400	6.0
600	6.5
800	6.8
1000	7.0
2000	7.9
3000	8.4
4000	8.7
6000	9.2
8000	9.5
10000	9.8

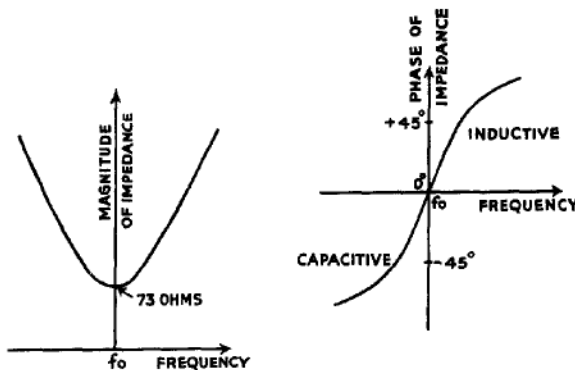


Fig.758.- Magnitude and phase of input impedance near resonance.

13. Factors Affecting the Resonant Length

As indicated previously, a centre-fed aerial in free space (o.g. suspended by fine strings from a high beam) is found to have a non-

reactive input impedance for a length rather less than  $0.5 \lambda$ . This appears to be due to the fact that the current distribution along the wire is not quite sinusoidal especially near the extremities. It is usually found that the non-reactive impedance occurs when the length is about  $0.48 \lambda$ . Curves of variation of  $R_r$  (for two values of the ratio wavelength to diameter) and  $X_r$  (for three values of the ratio) against length of aerial are given in Figs.759 and 760, respectively. Note that the radiation resistance varies, but not so critically as the reactance. This variation in resistance probably accounts for the fact that the values of  $Q$  given in Sec. 12, and based on a constant resistance, are 10% to 20% too low.

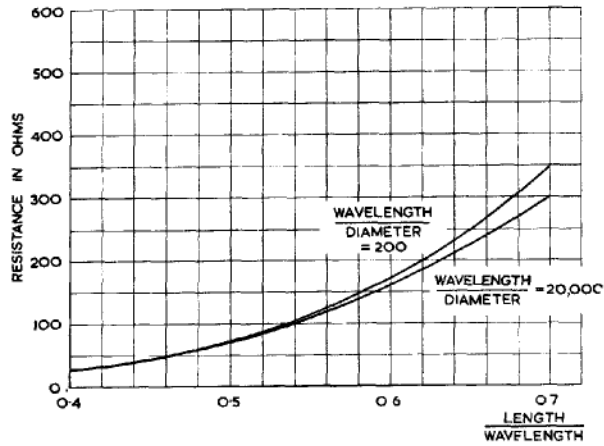


Fig.759.- Resistance of centre-fed aerial.

In practice insulators have often to be used, and it is clear that an insulator fixed to an aerial at a place where the current is high and voltage small has little effect on the aerial. Thus end-fed resonant length aerials are usually supported at their centres (Fig.756). An insulator fixed where the voltage is high will load the aerial like a condenser and make its effective length greater than its physical length. For this reason aerials are often cut shorter than the resonant length so as to allow for insulators at their extremities.

RECEIVING AERIALS

14. General

It is emphasised in Sec. 2 that the wave emitted from a transmitting aerial has a spherical wave-front but at large distances a small portion of the wave-front is effectively plane. Thus a receiving aerial is usually subject to the

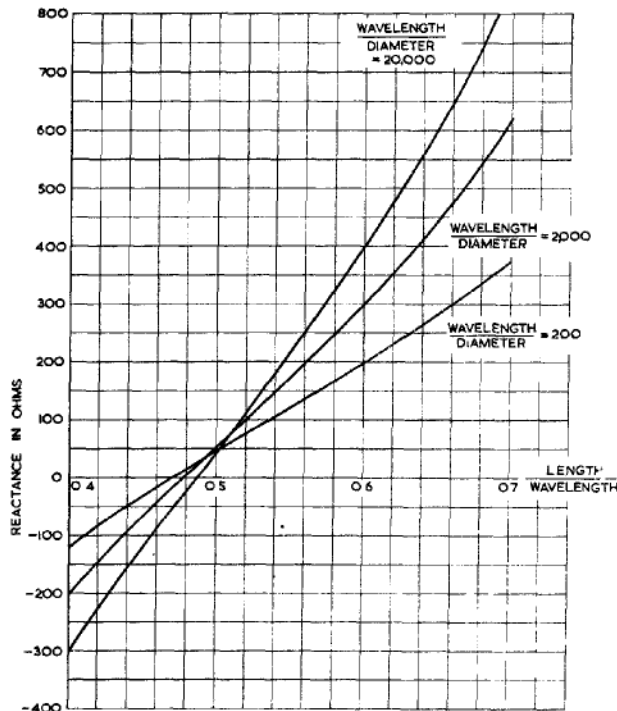


Fig.760.- Reactance of centre-fed aerial.

incidence of a plane electromagnetic wave. This wave sets up an EMF in the receiving aerial. The EMF for a given incident field strength depends on the direction from which the wave is incident, and a plot of this EMF against direction gives the field-strength diagram of the receiving aerial.

In order to utilise the EMF  $v$ , a load  $z_l$  is attached to the terminals of the aerial. Current then flows in the load. However, this current also flows in the aerial, which consequently radiates some power away. Thus the current  $i$  in the load is not equal to  $\frac{v}{z_l}$ , but is given by

$$i = \frac{v}{z_l + z_r} \dots\dots\dots (29)$$

where  $z_r$  is the impedance of the aerial. The equivalent circuit of the receiving aerial corresponding to equation (29) is shown in Fig.761. The useful power, i.e. the power in the load, is a maximum when the load is matched to the aerial impedance. This means, if the aerial has impedance  $R_r$ , that the load should be equal to  $R_r$ . If the aerial has a reactive component and impedance  $R_r + jX_r$ , then the load impedance should be equal to  $R_r - jX_r$ . (See Chap. 3 Sec. 4).

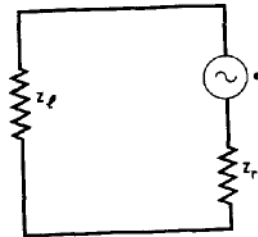


Fig.761.- Equivalent circuit of receiving aerial.

Under matched conditions, half the power is obtained in the load and half is re-radiated. In what follows it will always be assumed that the load is matched to the receiving aerial.

For a given incident field strength one is interested in how much power the aerial passes to the load. Owing to the non-uniformity of the field-strength diagram there is an optimum direction from which to have the wave incident. It is possible to compare matched receiving aerials by observing how much power is obtained in the load of each aerial when it is subject to a given incident field strength in its optimum direction. A hypothetical aerial which receives equally from all directions is taken as standard (Isotropic Receiver) and the ratio of the power picked up by the aerial to the power picked up by the isotropic receiver is the power gain of the aerial in reception.

Thus receiving aerials, like transmitting aerials, have a field-strength diagram, impedance and power gain. It has long been realised, almost intuitively, that these three properties of an aerial are the same when the aerial is used for reception and for transmission. A proof can be given, based on Maxwell's equations, and it is generally referred to as the Reciprocity Theorem.† In dealing with the properties of particular aerials one usually treats the aerial as a transmitter. The results are applicable also when the aerial is used for reception.

15. Power Relations for an Isotropic Receiving Aerial

The hypothetical isotropic receiving aerial is supposed to have a matched load attached to its terminals. If a plane wave of field-strength  $E$  RMS volts/metre is incident on the aerial, an EMF is set up in it and power is transferred to the load. As stated in Sec. 7, the power flow in the incident wave is (equation (17)),

$$P_a = \frac{E^2}{120\pi} \quad \text{watts/square metre} \dots\dots\dots (30)$$

Effectively, therefore, the aerial is intercepting some of this power and

† See Chap. 1 Sec. 7.

transferring it to the load. The aerial can therefore be represented by an area placed normal to the direction of the wave and of such a size that it intercepts the same amount of power as is found in the load. This is called the Effective Cross-Sectional Area of the aerial for absorption. Denoting it by  $A_o$  square metres, the power  $P_o$  in the load is given by :-

$$P_o = P_a A_o \text{ watts} \dots\dots\dots (31)$$

It can be shown that the effective cross-section of the isotropic absorber is given by the formula :-

$$A_o = \lambda^2 / 4\pi \text{ square metres} \dots\dots\dots (32)$$

Thus the power in the load of an isotropic receiving aerial under the incidence of a field  $E$  is from (30), (31) and (32) :-

$$\begin{aligned} P_o &= P_a A_o \\ &= \frac{E^2}{120\pi} \cdot \frac{\lambda^2}{4\pi} \\ &= \frac{E^2}{120} \left( \frac{\lambda}{2\pi} \right)^2 \text{ watts} \dots\dots\dots (33) \end{aligned}$$

**16. Power Relations for any Receiving Aerial**

Even the simplest aerial, the half-wave aerial, does not receive equally from all directions. In its best direction it has a power gain of 1.6 over an isotropic aerial. In general, if an aerial has a power gain  $g$ , and if the wave is incident from the best direction, then the power in the load is  $g$  times the power in the load of an isotropic receiving aerial subject to the same wave. Alternatively one may say that the effective cross section  $A$  of the receiving aerial is  $g$  times that of the isotropic receiver  $A_o$ . Hence we have

$$A = gA_o,$$

or, using (32),

$$A = \frac{g\lambda^2}{4\pi} \dots\dots\dots (34)$$

The power  $P$  in the load for an incident field strength  $E$  RMS volts/metre is given by

$$\begin{aligned} P &= P_a A \\ &= \frac{gE^2}{120} \left( \frac{\lambda}{2\pi} \right)^2 \text{ watts} \dots\dots\dots (35) \end{aligned}$$

Formula (34)(and also (32)) giving the effective cross-section for absorption by a receiving aerial is of great importance.

**17. TRANSMISSION AND RECEPTION**

The arguments of Secs. (9) and (16) enable one to solve the problem of calculating the power received from a distant transmitter Tx (Fig.762). Let the distance between transmitter and receiver be  $r$  metres. Let  $P_T$  be the transmitted power,  $g_T$  the gain of the transmitting aerial and  $g_R$  the gain of the receiving aerial. The power

passing through unit area of wavefront at distance  $r$  from the transmitter, in the best direction of the transmitting aerial, is

$$\frac{g_T P_T}{4 \pi r^2} \text{ watts/square metre} \dots\dots\dots(36)$$

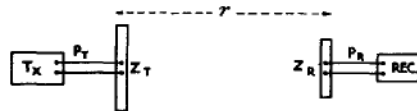


Fig.762.- Transmitter and receiver.

The effective absorption cross-section of the receiving aerial in its best direction is (see equation (34))

$$\frac{g_R \lambda^2}{4 \pi} \text{ square metres} \dots\dots\dots(37)$$

Hence the power  $P_R$  in the receiver is given by the product of (36) and (37) :-

$$P_R = P_T \frac{g_T \cdot g_R \lambda^2}{16 \pi^2 r^2} \text{ watts} \dots\dots\dots(38)$$

This power  $P_R$  is conveyed by feeder or waveguide to the receiver terminals (Fig.762). If the impedance looking into the receiver terminals is a resistance,  $R_i$  ohms, then the voltage  $V_R$  across the receiver terminals is given by

$$P_R = V_R^2 / R_i$$

or  $V_R = \sqrt{P_R R_i}$  RMS volts  $\dots\dots\dots(39)$

Example

A radio altimeter works on a frequency of 5,000 Mc/s., with a power output of  $\frac{1}{2}$  watt. The transmitting aerial has a gain of 100 and is fitted under the aircraft and directed vertically downwards. If the aircraft is flying at a height of 3,000 metres find what signal would be detected by a man on the ground equipped with an aerial whose gain is 500.

Using formula (38), or from first principles, we have

$$P_R = \frac{P_T g_T g_R \lambda^2}{(4 \pi r)^2}$$

Here  $P_T = \frac{1}{2}$ ,  $g_T = 100$ ,  $g_R = 500$ ,  $\lambda = 0.06$ ,  $r = 3,000$ .

Substituting, we find

$$P_R = \frac{(5 \cdot 10^{-1}) \cdot (10^2) \cdot (5 \cdot 10^2) \cdot (36 \cdot 10^{-4})}{(16 \pi^2)(9 \cdot 10^6)}$$

$$= \frac{25 \cdot 10^{-8}}{4} \text{ watts}$$

$$= 0.06 \text{ microwatts}$$

If the receiver input resistance is 80 ohms, what signal voltage would be obtained at the receiver ?

$$\begin{aligned} \text{We have } \frac{v^2}{80} &= \frac{25 \cdot 10^{-8}}{4} \\ v^2 &= 5 \cdot 10^{-6} \\ V &= 2 \cdot 2 \cdot 10^{-3} \text{ RMS volts} \\ &= 2 \cdot 2 \text{ RMS millivolts.} \end{aligned}$$

PROPAGATION AND RECEPTION OF SHORT WAVES

18. Scattering by an obstacle

Consider a metallic obstacle, such as an aircraft, in the path of a radio wave. The obstacle acts as a receiving aerial and intercepts part of the power in the wave. A receiving aerial is usually matched to a load (Sec. 4), in which case half of the power intercepted goes to the load and half is re-radiated. When there is no load, as in the case of a perfectly-conducting metallic obstacle, all the power intercepted is re-radiated. The re-radiated power may be picked up by a receiving aerial placed near the original transmitter and this arrangement is then an example of radar.

The obstacle acts as a kind of relay transmitter between the actual transmitter and receiver. In practice most obstacles have complicated field-strength diagrams, but for simplicity it has become the custom to consider each aspect separately, e.g., for an aircraft, the tail-on, head-on and side-on aspects. Focusing on one aspect one notes the power received and assumes then that the obstacle is transmitting back to the receiver like an isotropic radiator. This simplifies calculations.

The result is that an obstacle, in a given orientation relative to the radar station, is assumed to intercept some fraction of the power incident on it and to re-radiate this power back to the radar station as if the obstacle were an isotropic radiator. If P is the power per square metre in the incident wave expressed in watts/square metre and P watts is the power re-radiated by the obstacle (considered as an isotropic radiator) then the effective area of the obstacle, its Echoing Area (or Equivalent Echoing Area) is  $A_e$  square metres where

$$P = P_a A_e \dots\dots\dots (40)$$

(compare equation (31)).

In radar, the wavelength is usually small compared with the dimensions of the scattering obstacle. This being so, the echoing area  $A_e$  of a flat metal plate of area A normal to the wave is given by :-

$$A_e = 4\pi (A/\lambda)^2 \dots\dots\dots (41)$$

It increases as  $\lambda$ , the wavelength, is decreased. On the other hand, most obstacles such as aircraft are curved. In this case the beneficial effect of reduction in wavelength is neutralised by the curvature becoming more important at small wavelengths. On the whole there is no simple relationship between  $A_e$  and  $\lambda$ . For a medium bomber  $A_e$  is about 20 square metres for centimetre wavelengths.

Example

A radar set works on a wavelength of 10 cm with peak pulse

power of 100 kilowatts. The same aerial is used for transmitting and receiving, its gain being 250. The minimum power detectable by the receiver is  $10^{-12}$  watts. What is the maximum range of detection on a medium bomber?

The flux of power at range R metres from the transmitter is given (equation (36)) by

$$\begin{aligned}
 P_a &= \frac{g_T P_T}{4\pi R^2} \\
 &= \frac{250 \cdot 10^5}{4\pi R^2} \\
 &= \frac{6 \cdot 25 \cdot 10^6}{\pi R^2} \text{ watts/square metre.}
 \end{aligned}$$

The echoing area is assumed to be 20 square metres (see Sec. 18). Hence the power  $P_r$  re-radiated is

$$\begin{aligned}
 P_r &= \frac{6 \cdot 25 \cdot 10^6 \cdot 20}{\pi R^2} \dots\dots\dots (42) \\
 &= \frac{1 \cdot 25 \cdot 10^8}{\pi R^2} \text{ watts}
 \end{aligned}$$

If this is radiated isotropically, the power flux from the aircraft at the receiving aerial is

$$\frac{P_r}{4\pi R^2} \text{ watts/square metre} \dots\dots\dots (43)$$

The gain of the receiving aerial is 250, so its effective area is

$$\frac{250 \lambda^2}{4\pi}$$

i.e.  $\frac{6 \cdot 25}{10\pi}$  square metres  $\dots\dots\dots (44)$

The power received is the product of (43) and (44); i.e.,

$$\begin{aligned}
 &\frac{P_r}{4\pi R^2} \cdot \frac{6 \cdot 25}{10\pi} \\
 &= \frac{1 \cdot 25 \cdot 10^8}{4\pi^2 R^4} \cdot \frac{6 \cdot 25}{10\pi} \\
 &= \frac{6 \cdot 4 \cdot 10^5}{R^4} \text{ watts.}
 \end{aligned}$$

This is to be equal to the minimum detectable signal of  $10^{-12}$  watts. Thus

$$\frac{6 \cdot 4 \cdot 10^5}{R^4} = 10^{-12}$$

so that  $R^4 = 6 \cdot 4 \cdot 10^{17}$

and  $R = 28000 \text{ metres} = 28 \text{ km} \approx 17\frac{1}{2} \text{ miles.}$

**19. Range of a Radar Set**

The above example illustrates the method of calculating the maximum range of a radar set. The general formula is obtained as follows :-

Let  $P$  be the transmitted power in watts,  $\lambda$  the wavelength in metres, and  $g$  the gain of the aerial (used for transmitting and receiving). Then at range  $R$  metres the flux of power  $P_a$  is given by

$$P_a = \frac{gP}{4\pi R^2} \text{ watts/square metre} \dots\dots\dots (45)$$

(compare (22) and Sec. 9).

Now let the echoing area of the target be  $A_e$  square metres. Then the power  $P'$  re-radiated by the target is :-

$$\begin{aligned} P' &= P_a A_e \\ &= \frac{g^2 A_e P}{4\pi R^2} \text{ watts} \dots\dots\dots (46) \end{aligned}$$

The flux  $P'_a$  of power, back at the receiver, distant  $R$  metres from the target is

$$\begin{aligned} P'_a &= \frac{P'}{4\pi R^2} \\ &= \frac{g^2 A_e P}{(4\pi R^2)^2} \text{ watts/square metre} \dots\dots\dots (47) \end{aligned}$$

The effective cross-section  $A$  of the receiving aerial is given by (34), i.e.,

$$A = \frac{g \lambda^2}{4\pi} \text{ square metres.}$$

Thus the power  $P''$  received is

$$\begin{aligned} P'' &= AP'_a \\ &= \frac{g^2 \lambda^2 P A_e}{(4\pi)^3 R^4} \text{ watts.} \end{aligned}$$

If the minimum detectable power is  $\check{P}$ , then the maximum range of detection  $\hat{R}$  is given by the equation

$$\begin{aligned} \check{P} &= \frac{A_e P \lambda^2 g^2}{(4\pi)^3 \hat{R}^4} \\ \text{or } \hat{R} &= A_e^{\frac{1}{4}} \cdot (P/\check{P})^{\frac{1}{4}} \cdot \lambda^{\frac{1}{2}} \cdot g^{\frac{1}{2}} \cdot (4\pi)^{-\frac{3}{4}} \text{ metres} \dots\dots (48) \end{aligned}$$

The aerial is often a circular mirror of diameter  $2r$  and area  $\pi(2r)^2/4$ . For such a mirror it can be shown (equation (76)) that

$$\begin{aligned} g &= \frac{4\pi}{\lambda^2} \cdot \frac{\pi(2r)^2}{4} \\ g^{\frac{1}{2}} &= \frac{2\pi r}{\lambda} \end{aligned}$$

Thus we find that

$$\hat{R} = A_e^{\frac{1}{4}} \cdot (P/\check{P})^{\frac{1}{4}} \cdot 2r \cdot \lambda^{-\frac{1}{2}} \cdot (\pi/64)^{\frac{1}{4}} \text{ metres} \dots\dots (49)$$

It is remarkable that the maximum range increases only as the fourth root of the transmitted power. It is directly proportional to the diameter of the mirror.

20. Reflection from Ground and Sea

In most of the preceding sections it has been assumed that the aerial has been in free space, i.e., entirely independent of its position with respect to the ground or sea. It will be shown in the following sections that the field-strength diagram of any aerial can be considerably modified by reflections from the ground or sea. In order to investigate the behaviour of radio waves incident on the ground one must know the electrical properties of the earth. Consider a condenser made up from two metal plates with the space between filled with soil. The earth is not a very good insulator and the arrangement is most simply represented as a resistance or, better, a conductance  $G$  in shunt with a capacitance,  $C$ . When a high frequency alternating current is applied to the plates the admittance is given by

$$G + j \omega C \dots\dots\dots (50)$$

where  $\omega/2\pi$  is the frequency. It follows from expression (50) that for low frequencies the term  $G$  will be bigger than the term  $C$  and thus the earth behaves like a metal at low frequencies. On the other hand at sufficiently high frequencies  $\omega C$  will be bigger than  $G$  and the earth will behave as a dielectric.

The conductivity of the earth varies considerably depending on the dampness and type of the soil or rocks. However, when average values are substituted in (50) it appears that for all wavelengths used in radar, the  $\omega C$  term predominates and thus the earth can be considered to be a dielectric. The dielectric constant is generally taken to be 10.

Now consider the case of the sea. Again one takes a condenser with sea water between the plates and arrives at expression (50) for the admittance. The conductivity of the sea is much higher than that of land and the  $G$  term is therefore much larger. The frequency at which the conductive and susceptive terms of (50) are equal is approximately 1000 Mc/s (wave length 30 cm.). For frequencies well below this value the sea behaves like a metal whilst for much higher frequencies it behaves like a dielectric. Broadly speaking, on metre wavelengths the sea acts as a metal and on centimetre wavelengths the sea acts like a dielectric. The dielectric constant is 81.

21. Horizontally Polarised Waves Incident on Ground

As explained above, the ground acts as a dielectric for radar wavelengths. The incidence of a wave on the ground is thus similar to light falling on a glass surface. Part of the wave is reflected and part refracted. For normal incidence the well-known optical law,

$$\text{fraction reflected} = \frac{n-1}{n+1}$$

applies,  $n$  being the refractive index. The index of refraction of glass is 1.5 and of the earth 3.2 (square root of dielectric constant). Consequently, reflection of radio waves from the surface of the earth is more pronounced than that of light waves from glass.

Suppose now that the wave is polarised with the electric vector horizontal. At the point of incidence of the ray on the earth, we have

three electric fields  $\vec{E}$  (In),  $\vec{E}$ (Refrac) and  $\vec{E}$ (Reflec), for the incident, reflected and refracted rays. The two just above the surface must add together to equal the one just below the surface (Fig.763), i.e.



Fig.763.- Horizontally polarised radar waves incident on earth.

$$\vec{E}(\text{In}) + \vec{E}(\text{Reflec}) = \vec{E}(\text{Refrac}) \dots\dots\dots (51)$$

Owing to the high index of refraction, most of the wave is reflected and  $\vec{E}(\text{Refrac})$  is small, so that we have approximately, from (51),

$$\vec{E}(\text{Reflec}) = -\vec{E}(\text{In}) \dots\dots\dots (52)$$

There is thus a sudden phase change of about  $180^\circ$  on reflection and the reflection coefficient is practically unity. Reflection is most complete when the rays strike the surface at a small glancing angle, and falls off as one approaches normal incidence. The fraction reflected at normal incidence is about 50%.

22. Horizontally Polarised Waves Incident on Sea

Take first the case of centimetre wavelengths. As explained in Sec. 20, the sea then acts like a dielectric, and similar considerations arise as in the previous paragraph. Reflection is, however, more complete owing to the very high index of refraction, viz.  $\sqrt{81}$  or 9. Even at normal incidence the reflected ray is 90% the amplitude of the incident.

In the case of metre waves the sea behaves substantially metal. Take an incident and reflected wave as shown in Fig.764. The resultant electric field at the surface must be small (Chap. 5 Sec. 3). Hence the electric fields of the incident and reflected waves must be roughly equal and opposite. The reflection coefficient is about unity and there is a phase change of  $180^\circ$  on reflection.

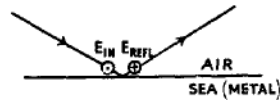


Fig.764.- Horizontally polarised metre waves incident on sea.

Thus, with horizontally polarised waves of any radar frequency, incident on the sea, the reflection coefficient can be assumed to be unity with a phase change of  $180^\circ$ . The sea is liable to be rough and, for short wavelengths, the roughness is of the same order as the radio wavelength. Reflection is not then specular and a definite reflected wave may not be found.

23. Reflection of Vertically Polarised Waves

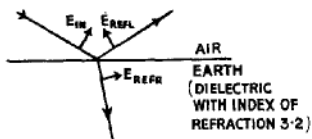


Fig.765.- Vertically polarised radar waves incident on earth.

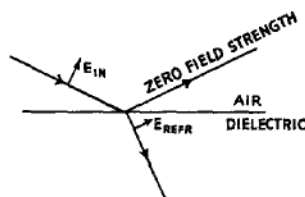


Fig.766.- Brewster angle.

The reflection of horizontally polarised waves discussed in Sec. 21 and 22 is comparatively simple, and the general result is that reflection is nearly always practically complete but with  $180^\circ$  phase change. When the electric field of the wave is vertical the situation is more complex. In this case the electric vectors in the incident, reflected and refracted waves are not parallel to the surface (Fig. 765) and the fitting together of the fields across the boundary is a comparatively difficult process.

Take first the case of any radar waves incident on the earth or of centimetre waves incident on the sea. The medium then behaves like a dielectric. At one particular angle of incidence the reflected and refracted rays are at right angles and the electric field E (Refrac) of the refracted wave is parallel to the direction of the reflected ray (Fig. 766). The electrons in the dielectric, oscillating under the influence of E (Refrac) radiate nothing along the direction of E (Reflec) and so the reflected wave is zero. This is the Brewster Effect, the appropriate angle of incidence being called the Brewster Angle. Measured from the horizontal it is about  $17^\circ$  for earth and  $62^\circ$  for sea. The Brewster effect will occur when the earth or sea is behaving like a dielectric, i.e., for all radar wavelengths incident on earth and for centimetre wavelengths incident on sea. At angles to the horizontal below the Brewster angle, the reflection takes place with phase reversal (Fig. 767); above the Brewster angle, without phase change (Fig. 768).

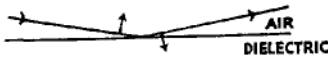


Fig.767.- Reflection of vertically polarised waves below Brewster angle (Note: The refracted ray is not shown).

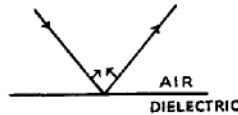


Fig.768.- Reflection of vertically polarised waves above Brewster angle (Note: The refracted ray is not shown).

In general, subject to certain reservations discussed in Sec.26, vertically polarised metre waves are reflected from the sea without phase change and with practically perfect reflection. The resultant field parallel to the surface at the point of incidence is zero, the sea acting like a metal for these wavelengths.

#### 24. Effect of Flat Earth on Field-Strength Diagram (Horizontal Polarisation)

Consider a horizontal half-wave aerial A placed height  $h$  above flat ground; (Fig. 769). Take a ray going off at an angle  $\alpha$  above the horizontal and another at an angle  $\alpha$  below the horizontal. These rays are equal in strength. The down-going ray hits the earth or sea and as indicated in Sec. 21 and 22 it may be assumed to suffer 100% reflection with  $180^\circ$  phase change if the angle of incidence is not near the perpendicular direction. At a far distant point P the direct ray AP and the indirect ray ABP come together and have to be added

vectorially. Draw AN perpendicular to the surface and produce to A' with A'N = AN and join A'B. Then from the Fig. 769,

$$A'B = AB.$$

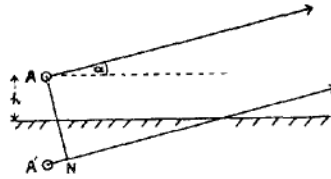
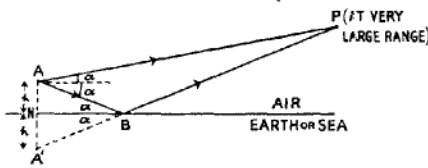


Fig.769.- Horizontal half-wave aerial and image. Fig.770.- Isotropic radiator and image.

Thus, so far as the path length is concerned, the ray ABP can be replaced by the path A'BP. Indeed one can put an Image source at A', consisting of another half-wave aerial fed with equal power and imagine the earth to be removed. Since the ray ABP suffers 180° phase change at B, the image source A' must oscillate 180° out of phase with A (Fig. 769 ).

Consider now an isotropic source a height h above a flat earth and radiating horizontally polarised waves. The image is a depth h below the earth. The field-strength diagram of the pair is found by taking a pair of parallel rays, from the source and its image, making an angle  $\alpha$  with the horizontal. The fields are added vectorially at a distant point. Referring to Fig.770, AN is drawn from the source A perpendicular to the lower ray. The path difference of the two parallel rays is A'N; in addition there is the fixed phase difference of 180° between source and image.

When the angle  $\alpha$  is very small the path difference A'N is also small and the total phase difference is 180° so that the resultant is zero. Thus no wave is propagated in the direction of grazing incidence along the earth's surface. As the angle  $\alpha$  is gradually increased from zero the total phase difference between the two rays increases from 180° towards 360°, at which the two rays are in phase and reinforce. This condition arises when A'N is  $\lambda/2$ . For a given  $\lambda$ , if the distance 2h between the source and image is very large,  $\alpha$  the angle need not increase greatly from zero in order to make A'N =  $\lambda/2$ . The bigger the base-line, so to speak, the sooner the path difference develops.

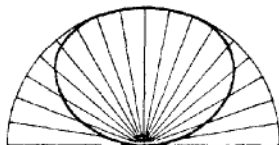


Fig.771.- Field Strength diagram for aerial distance  $\lambda/4$  above earth.

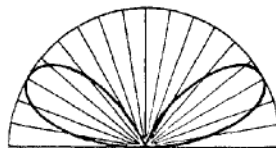


Fig.772.- Field Strength diagram for aerial distance  $\lambda/2$  above earth.

To take a few examples, suppose  $h = \lambda/4$ , then  $\alpha$  must increase to  $90^\circ$ , with the rays shooting straight up, before a total phase difference of  $360^\circ$  is achieved. The field-strength diagram in polar co-ordinates is then as shown in Fig. 771. When  $h = \lambda/2$ , the phase difference is  $180^\circ$  for rays shooting straight up, and the field strength diagram is as illustrated in Fig. 772. As the height is increased, more and more lobes appear, there being a lobe between  $0^\circ$  and  $90^\circ$  for every  $\lambda/2$  of height above the ground. These are often called Interference Lobes. For an aerial system  $7\lambda$  above the earth there will be 14 lobes as shown in Fig. 773. The lobes at low angles are approximately equally spaced in angle and occur at  $2^\circ, 6^\circ, 10^\circ, 14^\circ \dots$  but at high angles the angular spacing opens up, with the lobes more widely separated. For  $14\lambda$  height above the ground, the first lobes would be at  $1^\circ, 3^\circ, 5^\circ, 7^\circ \dots$  and so on. The angular difference between the lowest lobes is inversely proportional to the height of the phase-centre of the aerial system.

When the beaming of the aerial system is not too strong, so that the first interference lobe occurs near the maximum of the free-space field-strength diagram, the field strength at a given distance in the direction of the first lobe is twice the free-space value. Thus by equation (25) the power gain  $g$ , of the system is four times the power gain of the aerial in free space and the maximum range of detection of a ground radar system is twice the free space value; (see equation (48)).

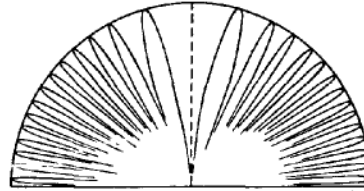


Fig. 773.- Field Strength diagram for aerial distance  $7\lambda$  above earth.

#### 25. Effect of Flat Earth on Field Strength Diagram (Vertical Polarisation)

From the results of Sec. 24 and 23 we deduce the following facts for vertically polarised radar waves incident on ground. Up to the Brewster angle ( $17^\circ$ ), the effects are similar to those for horizontally polarised waves, with lobes depending on the height of the aerial system above the ground and as in Sec. 24. Near the Brewster angle the reflected ray disappears. Above the Brewster angle reflection takes place without phase change, and broadly speaking, maxima and minima in the field-strength diagram are interchanged from their positions in the horizontally polarised case (Fig. 774).

For vertically polarised centimetre waves incident on a smooth sea the same results hold but the Brewster angle is now  $62^\circ$ .

For vertically polarised waves of several metres in wavelength incident on the sea, there is no phase change on reflection. The maxima and minima of the horizontally polarised case are here interchanged and, in particular, there is a lobe at sea level (Fig. 775).

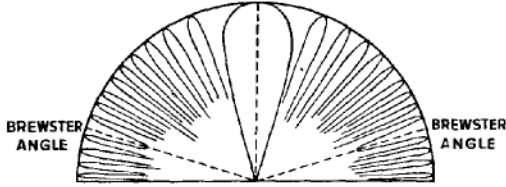


Fig.774.- Field Strength diagram (vertically polarised waves) for aerial distance  $7\lambda$  above earth.

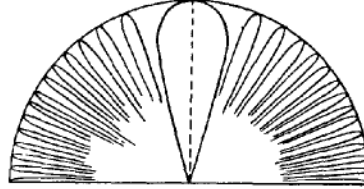


Fig.775.- Field Strength diagram (vertically polarised metre waves) for aerial distance  $7\lambda$  above sea.

26. Summary of Effect of Flat Surface

The following table shows the lobes in the vertical field-strength diagram of an isotropic radiator placed  $14\lambda$  above earth or sea and summarises the results of the two preceding paragraphs :-

<u>Polarisation</u>	<u>Wavelength</u>	<u>Surface</u>	<u>Lobes</u>
Horizontal	Any radar	Land	$1^\circ, 3^\circ, 5^\circ$ and so on.
Horizontal	Any radar	Sea	$1^\circ, 3^\circ, 5^\circ$ and so on.
Vertical	Any radar	Land	$1^\circ, 3^\circ, 5^\circ$ up to $17^\circ$ then change over to $18^\circ, 20^\circ, 22^\circ$ and so on.
Vertical	Centimetre	Sea	$1^\circ, 3^\circ, 5^\circ$ up to $6\frac{1}{2}^\circ$ then change over to $8^\circ, 10^\circ, 12^\circ$ and so on.
Vertical	Metre	Sea	$0^\circ, 2^\circ, 4^\circ, 6^\circ, 8^\circ$ and so on.

The free-space field-strength diagram is split up into lobes depending on the height of the phase centre above the earth's surface. Mathematically, the free-space field-strength factor must be multiplied by

$$\sin \left[ \frac{360^\circ h \sin \alpha}{\lambda} \right] \dots\dots\dots (53)$$

or

$$\cos \left[ \frac{360^\circ h \sin \alpha}{\lambda} \right] \dots\dots\dots (54)$$

according to whether there is or is not change of phase at reflection. Although the maximum range of detection is increased by the presence of the lobes, the zeros in between the lobes give gaps in the radar coverage.

Generally speaking, reflection is more complete and the formation of maxima and minima is more straightforward with horizontally polarised than with vertically polarised waves. With the metre waves used in radar, one is inevitably working over the wavelength band in which the sea is changing from a "metal" to a "dielectric". This changeover does not take place suddenly and so the simple treatment given above shows only the essential details of the effect of the sea on vertically polarised waves.

To take an example, suppose we are dealing with 3-metre waves, vertically polarised, and incident on the sea. A detailed investigation shows that there is a pseudo-Brewster angle at  $2^\circ$ . The lobe at sea level is thus unlikely to be well developed. For wavelengths of a metre and upwards this pseudo-Brewster angle is inversely proportional to the square root of the wavelength - at 30 metres it would be about  $2/3^\circ$  - and only on quite long wavelengths will the sea give exactly the effects of a good conductor at very low angles of elevation.

The choice of polarisation for a coastal or sea-borne radar using metre waves to detect low-flying aircraft has been a matter of some controversy. Observations show that with vertical polarisation there is considerable sea-clutter (i.e., scattering back from sea-waves) up to ranges of about 20 miles, but with horizontal polarisation sea clutter is small. On the other hand the ranges of detection of low-flying aircraft are about the same for either polarisation. It appears therefore that there is more field strength at sea level with vertically polarised waves, but a little above the sea the field strength of horizontally polarised waves soon becomes appreciable. The results obtained clearly depend on the height of the aerials above the sea, and the matter is thus further complicated. Most British radar sets for aircraft and ship detection use horizontally polarised waves.

#### 27. Gap Filling

One method of filling the gaps in the vertical field-strength diagram is to employ two aerial systems at different heights above the ground. These can be arranged so that many of the gaps in one field-strength diagram are filled by the lobes of the other and, by switching as required, a target may be followed continuously.

Another method is to use a combined array of vertically and horizontally polarised aerials. From the previous paragraphs the maxima and zeros are interchanged for angles above the Brewster angle when the polarisation is changed.

#### 28. Effect of Earth's Curvature : Refraction

Consider an aerial system A at height  $h$  feet above the earth's surface. The earth is approximately a sphere of radius 4,000 miles and the geometric horizon for this aerial system is at the point P in Fig. 776. Although radio waves of large wavelength are diffracted easily round the earth's curvature, short waves as used in radar do not diffract

appreciably into regions beyond and underneath the optical horizon.

Strictly speaking the horizon is slightly more distant for radio waves than the geometric point in Fig.776. This is due to the fact that these waves are bent or refracted in the earth's atmosphere.



Fig.776.- Optical horizon.

Under normal conditions, the dielectric constant of air is 1.00055. Higher up in the atmosphere the air becomes less dense and the dielectric constant approaches more nearly to unity. Thus a ray travelling up into the atmosphere is continually passing from more dense to less dense regions in the optical sense. In accordance with the principles of refraction, the ray is therefore continually bent away from the normal. The effect is very small but is made more appreciable by the presence of water vapour in the atmosphere. Owing to its molecular structure, water vapour has a dielectric constant of 1.01 at normal temperature. Thus, although the amount of water vapour in the atmosphere is only 1.4%, its efficacy as a refracting medium is comparable with that of the air itself. The percentage of water vapour decreases as one ascends into the atmosphere so that again we have the effect of bending the radio rays. A ray starting out at a small angle to the horizontal is therefore slowly bent round and can reach a point more distant than the geometric horizon. It is found that this can be allowed for approximately by assuming the radius of the earth to be 6,000 miles instead of 4,000.

The effect just described is normal refraction. Occasionally in tropical climates the water vapour content is high, and varies very rapidly with height. In this case Super-Refraction takes place, the rays may even bounce several times from the earth's surface, and considerable penetration takes place into the region beyond and beneath the geometrical horizon. This phenomenon is also termed Anomalous Propagation or briefly Anoprop.

#### COMMON TYPES OF AERIAL ARRAYS

##### 29. Broadside Array

An array is an aerial system built up from a number of elements, and arranged to give a field-strength diagram of some desired form. In the case of a broadside array the elements are arranged in a plane so as to give a sharply beamed lobe in a direction normal to the plane of the array. The elements are usually half-wave aeriels and such arrays are mainly used on metre wavelengths. As described in Sec. 4 a half-wave aerial radiates a spherical wavefront with the mid-point of the aerial as phase centre, i.e., as centre of the sphere. The field strength varies, at a given distance, according to  $E_0 D(\theta)$ , given in equation (9), in the plane of the aerial. In working out the field-strength diagram of an array it is convenient and correct to ignore this field strength variation in the first place and simply replace each half-wave aerial by an isotropic radiator or "point source" placed at the mid-point. The correction factor (9) can then be introduced when the field-strength diagram of the array of isotropic sources has been evaluated.

##### 30. Linear Broadside Array

This is a broadside in which there is only a single row or column of elements fed in phase. The array may take four different forms

in practice according as the elements are horizontal or vertical and stacked vertically or horizontally. The four cases are illustrated in Figs.777 to 780. Replacing the elements by point radiators as explained in the previous paragraph, one obtains either a row or column (i.e., a line), of point radiators.



Fig.777.- Vertical stack.



Fig.778.- Vertical line.

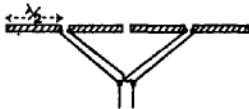


Fig.779.- Horizontal line.

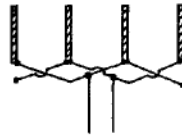


Fig.780.- Horizontal row.

The field-strength diagram of such a line of isotropic radiators is obtained by adding up the waves, sent out in any direction, from all the radiators. In this section we shall limit discussion to arrays in which all the elements are equally energised.

Consider first the field-strength diagram in the plane through the line of radiators, i.e., the plane of the paper in Fig.781. Take parallel rays going out from each radiator making an angle  $\theta$  with the normal direction. Consider the ray from the centre radiator as standard if the number of elements is odd; if the number is even, introduce as standard a further hypothetical ray from the geometrical centre of the line of elements. Now the rays from the elements can be grouped in pairs on either side of the standard, one ray of the pair leading and the other lagging, by the same amount, on the standard. Such a pair is indicated by AB, CD in Fig.781 with phase lead GF and phase lag CJ respectively. By the same argument as in Sec. 4 (See Fig.748) the resultant field from such a pair has the same phase as the standard ray. Thus, the phase centre of the array is its mid-point. At a great distance it appears as if a spherical wavefront were spreading out from this point.

The variation of the strength of the wave as the direction  $\theta$  varies is found by adding up all the rays. This is conveniently done simply by taking them in turn from left to right and adding vectorially. The vector addition can be done either graphically or algebraically. The result

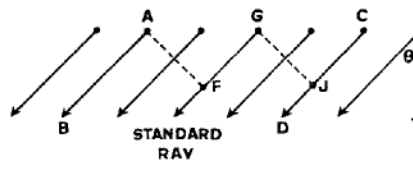


Fig.781.- Line of isotropic radiators.

depends on the spacing between the point radiators. This spacing is nearly always  $\lambda/2$  in practice, and the field-strength diagram is then given by :-

$$E \propto \frac{\sin [90^\circ n \sin \theta]}{\sin [90^\circ \sin \theta]} \dots\dots\dots (55)$$

where n is the number of elements in the array. Expression (55) is often called the Beaming Factor and sometimes the Grating Factor. Denoting it by B( $\theta$ ) we have therefore :-

$$B(\theta) = \frac{\sin [90^\circ n \sin \theta]}{\sin [90^\circ \sin \theta]} \dots\dots\dots (56)$$

This is plotted for n = 2, 4, 6 and 10 in Figs 782, 783, 784, and 785. It must be multiplied by the field-strength factor of the individual element in this plane in order to obtain the actual field-strength distribution of the array.

The field-strength factor for the array, in a plane through the centre of the line of elements and perpendicular to its length (i.e. a plane through G in Fig. 781 and perpendicular to AGC is constant. There is no change in the field strength as one goes round the line of isotropic sources at a constant distance in this plane. In the case of the actual array, however, the field-strength factor of each individual element must be multiplied in.

Referring to the arrays illustrated in Figs. 777, 778, 779 and 780, it is now possible to obtain their field-strength diagrams in the two planes in terms of B, given by (56), and D, given by (9). The E-plane is taken as the  $\theta$ -plane and H-plane as the  $\phi$ -plane in accordance with Sec. 3.

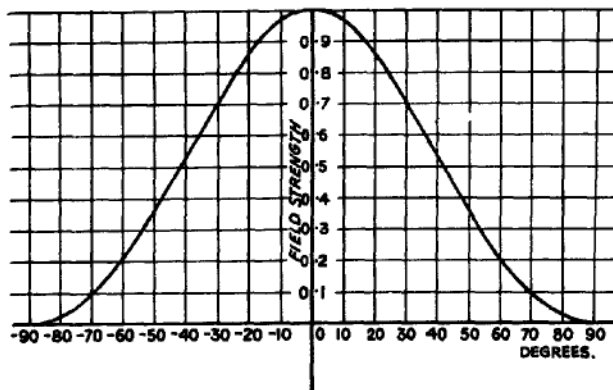


Fig. 782. - Beaming factor for two aerials spaced  $\lambda/2$  apart.

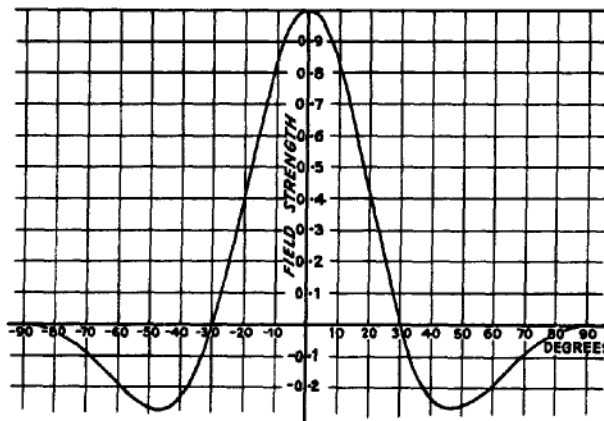


Fig. 783. - Beaming factor for four aerials spaced  $\lambda/2$  apart.

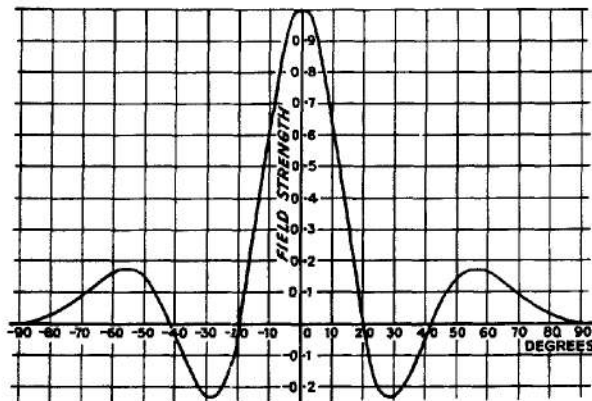


Fig. 784.- Beaming factor for six aerials spaced  $\lambda/2$  apart.

<u>Figure</u>	<u>Description</u>	<u>Plane</u>	<u>Resultant Field-Strength Factor</u>
777	Horizontal Half-Wave Aerials in Vertical Stack with Half-Wave spacing.	Vertical or H-plane	$B(\phi)$ ( $B(\theta)$ means that $\theta$ in equation (56) is replaced by $\phi$ .)
-do-		Horizontal or E-plane	$D(\theta)$
778	Vertical Half-Wave Aerials in Vertical Stack tip-to-tip.	Vertical or E-plane	$B(\theta).D(\theta)$
-do-		Horizontal or H-plane	constant
779	Horizontal Half-Wave Aerials in Horizontal Row tip-to-tip	Vertical or H-plane	constant
-do-		Horizontal or E-plane	$B(\theta).D(\theta)$
780	Vertical Half-Wave Aerials in Horizontal Row with Half-Wave spacing	Vertical or E-plane	$D(\theta)$
-do-		Horizontal or H-plane	$B(\phi)$

If elements other than half-wave aerials, but yet possessing axial symmetry, are employed, then the above table can be applied provided  $D(\theta)$  is replaced by the appropriate field-strength factor. The main features of the beaming factors shown in Figs 782, 783, 784, and 785 are as follows :- There is a large maximum or Main Beam in the direction at right angles to the line of the array. The direction of this maximum

is sometimes called the Line of Shoot. Besides this there are a number of smaller maxima or Side Lobes.

The phase jumps  $180^\circ$  as the angle varies through the position of zero amplitude from one side-lobe to the next. An exception may occur between adjacent lobes at right angles to the main beam. The width of the main beam decreases as the number of elements increases. The Beam Width is usually defined as the number of degrees across the beam at half-maximum amplitude. This is plotted as a function of the number of elements in Fig.786. A rough rule, valid for a large number of elements, is

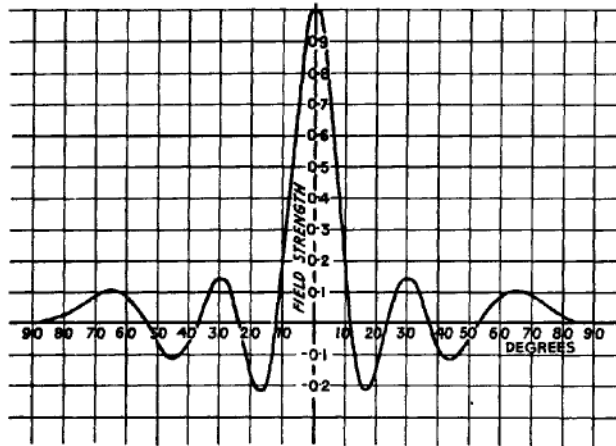


Fig.785.- Beaming factor for ten aeriels spaced  $\lambda/2$  apart.

$$\text{beam width in degrees} = \frac{70 \times \text{wavelength}}{\text{width of array}} \dots\dots\dots (57)$$

The field-strength diagram of the individual elements, being rather broad, (Fig.749) hardly affects the beam-width when the number of elements is large.

When the number of elements is large, the first side-lobe is about 21% of the amplitude of the main maximum.

The gain (equation (65)), as can be shown by arguments given later, is about three times the length of the array expressed in wavelengths.

The choice of the aerial system for any particular function can be made from the table above. A

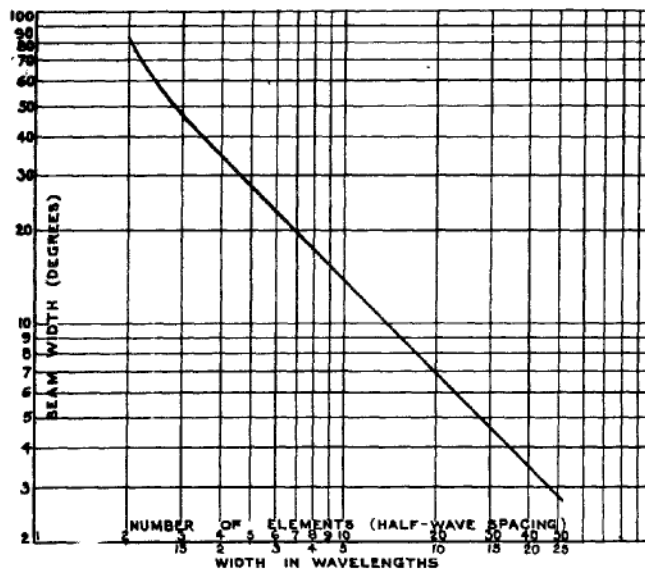


Fig.786.- Beam width of broadside.

beacon aerial, required to radiate all round and beamed in the vertical plane to prevent radiation being wasted by going vertically up into the sky would be best taken from Fig. 778. An aerial required to receive signals from a particular direction but from aircraft at any height would be as illustrated in Fig.779 or Fig.780

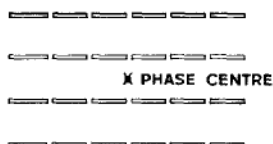


Fig.787.- Complete broadside with horizontal polarisation.

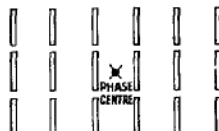


Fig.788.- Complete broadside with vertical polarisation.

**31. Complete Broadside Array**

The complete broadside has elements in columns and rows fed equally and in phase. The elements will usually be half-wave aeri- als arranged either horizontally (Fig.787 ) or vertically (Fig.788 ), with centre spacing  $\lambda/2$ . To obtain the field-strength diagram of the broad- side one first replaces the elements by point sources as in the previous paragraph. One then takes, say, a horizontal row of point sources and finds its beaming factor  $B_h(\theta)$ , by the method adopted for the linear array. Its phase centre is at its mid-point so that the whole hori- zontal row may itself be replaced by a point source at its mid-point radiating a spherical wavefront and with beaming factor  $B_h(\theta)$  in the horizontal plane and constant in the vertical plane. Doing the same for all the horizontal rows, one finishes with a vertical line of point radiators. Assume now that these radiate isotropically. The phase centre is at the mid-point, i.e., at the centre of the whole array. The beaming factor in the horizontal plane is constant. In the vertical plane there is a beaming factor  $B_v(\phi)$ . For the whole array one takes the product of all the factors. Hence for horizontal polarisation we find :-

	Half-Wave Aerial	Horizontal Row	Vertical Row	Whole Array
Horizontal Plane	$D(\theta)$	$B_h(\theta)$	constant	$D(\theta) \cdot B_h(\theta)$
Vertical Plane	constant	constant	$B_v(\phi)$	$B_v(\phi)$

The corresponding results for vertical elements are obtained by reading "vertical" for "horizontal" and vice versa everywhere in the above table.

If there are n elements in a horizontal row and m elements in the vertical column, with  $\lambda/2$  spacing between centres, then

$$B_h(\theta) = \frac{\sin(90^\circ n \sin \theta)}{\sin(90^\circ \sin \theta)} \dots\dots\dots (58)$$

and

$$B_v(\theta) = \frac{\sin(90^\circ \pm \sin \theta)}{\sin(90^\circ \sin \theta)} \dots\dots\dots (59)$$

The field-strength diagrams of Figs 782, 783, 784 and 785 can thus be used to find the horizontal and vertical beaming factors of the complete broadside. When the beaming is great, with a large number of elements, the  $D(\theta)$  factor of the individual elements hardly affects the beam width.

This type of aerial, the complete broadside, is used to obtain greater beaming in the two planes than is possible with a linear array.

32. Use of Reflecting Screen behind Broadside Array

The broadside arrays described above radiate both in front and behind as shown in Fig. 789. This is objectionable for most radar purposes and a reflecting metal screen may be positioned behind the array. This has the effect of blocking out the backward radiation. In order to investigate the effect of the screen in greater detail



Fig. 789.- Broadside without reflector (polar plot).

consider a single half-wave aerial a distance  $a$  in front of a metal sheet; (Fig. 790). As is well known, there can be no electric field along the surface of a good conductor (this is sometimes referred to as a boundary condition). Hence there can be no electric field along the line AB in Fig. 790.

Now remove the metal sheet and place a half-wave aerial a distance  $2a$  from the first, fed with the same power but driven anti-phase (Fig. 791). At a point P on the line AB there is an electric field  $E$  due to each dipole and because of the anti-phase relationship these are as shown in the diagram.

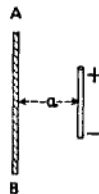


Fig. 790.- Aerial and metal reflector.

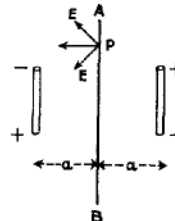


Fig. 791.- Aerial and image.

Their resultant is at right angles to AB, i.e. the electric field due to this combination is zero along AB. Thus the field is zero along AB in both cases Fig. 790 and Fig. 791. By such arguments it follows that, so far as the field to the right of the screen is concerned, the two arrangements are equivalent. This is indeed just the principle of images, well known in optics and already discussed in Sec. 24.

Now consider the broadside array with a metal screen behind it. The phase centre of the broadside without the screen is at the centre of the array; (Sec 31). Replace the metal reflecting screen by an image source, anti-phase but of the same strength (Fig. 792). The radiated field to the right of the array with screen is obtained by multiplying the field-strength factor of these two anti-phase isotropic sources by the beaming factor of the array alone. The beaming factor of the array

is already known from Sec. 31. The field-strength factor of the pair of antiphase sources depends on their distance apart,  $2a$ . In practice  $a$  is usually  $\lambda/8$  so that the source and its image are  $\lambda/4$  apart. The field-strength diagram of such an arrangement can be given by the formula :-

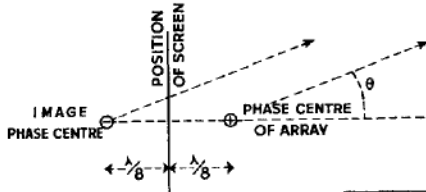
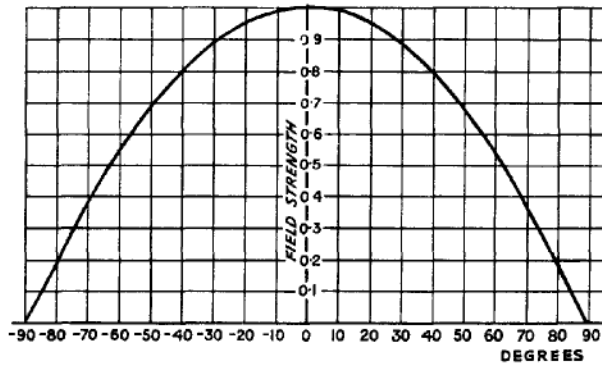


Fig.792.- Array with image.

Fig.793.- Beaming factor due to metal sheet placed  $\lambda/8$  behind array.



$$E \propto \sqrt{2} \sin(45^\circ \cos \theta) \dots\dots\dots (60)$$

which is plotted in Fig.793. Due to this factor there is a slight sharpening of the beam, and a slight reduction in side lobes, because of the reflecting screen. The phase centre of the arrangement is in the plane of the screen. Formula (60) applies only in front of the screen, i.e., from  $\theta = -90^\circ$  to  $\theta = +90^\circ$ . Behind the screen the field is always zero. Finally it is emphasised that the beaming given by (60) applies not only in the  $\theta$ -plane but in all planes normal to the screen.

**33. Wire Netting Reflector Screens**

In practice, a complete metal sheet is objectionable since it would have a high windage area. The reflecting screen is normally made of wire netting. Some radiation thus leaks through the back of the screen. Suppose the screen to be made of wires placed vertically and horizontally, forming a square or rectangular network. It appears then that the wires effective in reflecting back the wave are those lying parallel to the electric field, and the spacing and thickness of these wires is the determining factor in judging how much radiation leaks through. Let the wires parallel to the electric field be of diameter  $d$  and spaced  $s$  apart; (Fig.794). Then the amplitude of the electric field leaking through the netting is given, approximately, as a fraction of the incident electric field, by the expression :-

$$\frac{2s}{\lambda} \cdot \log_{\epsilon} \left( \frac{s}{\pi d} \right) \dots\dots\dots (61)$$

the quantities  $s$ ,  $\lambda$  and  $d$  all being expressed in the same units. The factor  $2s/\lambda$  shows that the main requirement to ensure small leakage is that the spacing  $s$  of the wires shall be quite small compared with the wavelength. In addition, the logarithmic factor shows that thick wires are preferable to thin ones. Wire netting is often made with a hexagonal mesh and, due to the method of twisting together, some sets of wires are thicker than others; (Fig.795). Clearly this netting should be oriented so that the thick wires are parallel to the electric field.

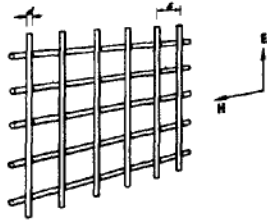


Fig.794.- Wave incident on wire netting.

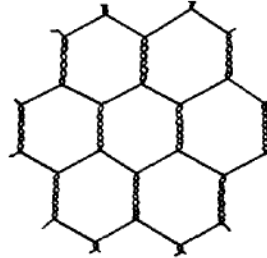


Fig.795.- Hexagonal wire netting.

As an example of formula (61), to give orders of magnitude, let us assume

$$s = \frac{1}{2}'' , d = 1/16'' \text{ and } \lambda = 60'' . \text{ Then}$$

$$\begin{aligned} \frac{E(\text{leakage})}{E(\text{incident})} &= \frac{2 \cdot \frac{1}{2}}{60} \cdot \log_{\epsilon} \left( \frac{\frac{1}{2}}{\pi \cdot \frac{1}{16}} \right) \\ &= \frac{1}{60} \cdot (0.95) \\ &= 1.6 \text{ per cent.} \end{aligned}$$

If  $d = 1/32''$ , the answer is 2.7 per cent. The wire must be a reasonably good conductor for RF and thus iron wire should not be used unless coated over completely by some other metal such as zinc or tin.

In theory, a reflecting screen behind an array should be infinite in extent. If it is not sufficiently extended beyond the aerials at the sides of the array, radiation will leak round the edges of the screen and shoot out behind. In practice it appears that the screen need not extend more than  $\lambda/2$  beyond the centre points of the outermost half-wave aerials, and indeed an extension of only  $\lambda/4$  from the centres of these aerials is often found in practical installations, without, apparently, resulting in any appreciable loss.

#### 34. Power Gain of Broadside Array

Since a broadside of half-wave aerials has a considerable beaming in its field-strength diagram, the power gain is high. The calculation of the power gain by the method of integration of power flow across a sphere is difficult. An approximate answer can be obtained as follows:-

Assume that  $R_r$  is the radiation resistance and  $I$  the RMS current, both measured at the centre of each half-wave aerial. (In practice all the aerials do not have the same radiation resistance due to mutual coupling. Neglect of this variation does not appreciably affect the accuracy in most cases). The power in each aerial is  $I^2 R_r$  and, if there are  $N$  aerials altogether in the broadside, the total power  $P$  is given by

$$P = NI^2 R_r \dots\dots\dots (62)$$

At a distant point in the best direction, the fields from all the aerials in the array add up together. The array thus gives the same field at this point as would arise from a single aerial carrying current  $NI$  at its centre, i.e., supplied with power  $P'$  given by

$$P' = (NI)^2 R_r \dots\dots\dots (63)$$

Thus the power gain  $g_1$  of the array relative to the half-wave aerial is given by

$$\begin{aligned} g_1 &= P'/P \\ &= N \dots\dots\dots (64) \end{aligned}$$

The power gain  $g$  relative to an isotropic radiator will (by Sec. 10) be  $1\frac{1}{2}$  times this, i.e.,

$$g = 3N/2 \dots\dots\dots (65)$$

If a reflecting sheet is used behind the array, the gain is approximately doubled, so that finally, for a broadside of  $N$  aerials with reflecting screen,

$$g = 3N \dots\dots\dots (66)$$

The effective cross-sectional area  $A$  of an array of  $N$  aerials with  $\lambda/2$  spacings is rather indefinite since the reflecting screen projects beyond the aerials. With the practical extensions of the screen discussed in Sec. 33, each aerial, including the outermost ones, is accounting for an area  $\lambda/2$  square. Thus, assuming that this still holds for each aerial in the array,  $A$  is given by :-

$$\begin{aligned} A &= N \left(\frac{\lambda}{2}\right)^2 \dots\dots\dots (67) \\ &= N \frac{\lambda^2}{4} . \end{aligned}$$

Substituting for  $N$  in (66) and (67) we obtain

$$g = \frac{4 \cdot A \cdot 3}{\lambda^2} .$$

A more accurate calculation, for a large broadside, gives

$$g = \frac{4 \pi A}{\lambda^2} \dots\dots\dots (68)$$

and this latter is the formula which should be used. It will readily be apparent that these results depend rather much on the assumption of  $\lambda/2$  centre-to-centre spacing between the aerials. It appears that this is a reasonable spacing to adopt and very small or very large spacings should be avoided. With close spacing, interaction between aerials becomes more pronounced and nullifies the increase in gain which would otherwise be expected. For spacing much greater than  $\lambda/2$  side lobes are introduced with a consequent waste of energy.

The general idea of the "area approach" to broadside arrays should be noted :-

A given area or aperture  $A$  is available from space, mobility and other considerations. It should then be possible to obtain a power gain  $g$  given by the equation (68). This is done by filling the space with half-wave aerials placed about  $\lambda/2$  apart and backing the space by a

reflecting screen; (Fig.796 ). The beam width in the horizontal plane is dependent on the horizontal width of the array, and in the vertical plane dependent on the vertical dimension.

35. Feeding Arrangements for Broadside Arrays

The first requirement in feeding a broadside array is to ensure that the elements are radiating in phase. This will be so if the elements are placed at intervals of  $\lambda/2$  along the feeder, provided it is an open wire feeder and that the feeder is crossed over between each aerial. The velocity of propagation in polythene-filled feeders is about  $2/3$  that in free-space and  $\lambda$  in such a feeder is  $2/3$  of the free-space wavelength, and allowance must be made for this. The next requirement is to obtain reasonable matching between the aeriels and feeders. Centre-fed half-wave aeriels are unsuitable because, when several are paralleled, the load on the feeder is small ( $73/N$  ohms, where  $N$  is the number of aeriels.) Most open wire feeders have a characteristic impedance of from 300 to 600 ohms. It is therefore more convenient to end-feed the half-wave aeriels (Sec. 11) and so obtain loads of the order of the feeder impedance. A slight mismatch can be removed by the use of stubs. In practice, therefore, broadside arrays are often built up in bays - each bay consisting of two stacks of half-wave aeriels, end-fed (Fig.797). The bays must all be fed in phase and with the same amount of power. This is ensured by careful cutting of the feeder lengths and by matching each bay to its feeder.

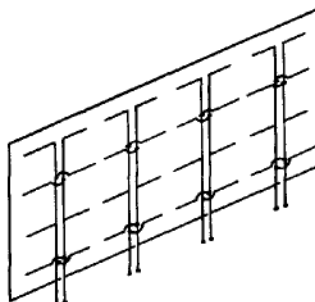


Fig.796.- Schematic diagram of broadside array backed by reflector sheet.

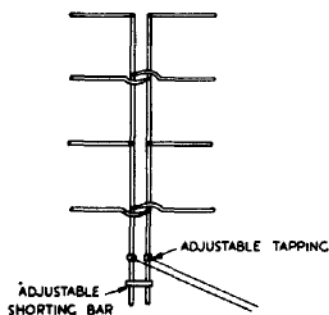


Fig.797.- Bay of half-wave aeriels.

The input resistance of a pair of half-wave aeriels has been given in Sec. 11. However, due to coupling between the aeriels and the proximity of the reflecting screen, the input resistance may differ considerably from the free-space value. This neglect of interactions between the aeriels affects the theoretical arguments of Sec. 34, but the final results (65) and (68) are probably not far wrong owing to compensating factors.

36. Example of a Complete Broadside Array

A broadside array measures 25' x 10' and consists of 40 half-wave aeriels arranged with  $\lambda/2$  spacing between their centres, the wavelength being 5'. The array is backed by a metal reflecting screen. Find the power gain and the beam widths in the two principal planes.

From (68) we have

$$\begin{aligned}
 g &= \frac{4 \pi A}{\lambda^2} \\
 &= \frac{4 \cdot \pi \cdot 25 \cdot 10}{5^2} \\
 &= 126 \\
 &\text{or } 20 \text{ db.}
 \end{aligned}$$

In the plane through the long dimension there are ten aeri-als in a line and hence from (57)

$$\begin{aligned}
 \text{beam width} &= \frac{70.5^\circ}{25} \\
 &= 14^\circ.
 \end{aligned}$$

Alternatively the same result may be obtained from Fig.786 .

In the plane through the short dimension there are four aeri-als in a line and, from Fig.796, the beam width =  $34^\circ$ .

$$\text{Formula (57) gives } \frac{70 \times 5}{10} = 35^\circ.$$

37. Tapered Feed to Linear Broadside Arrays

Returning to a consideration of a line of radiators (see Sec.30) the field-strength diagrams shown in Figs.782, to 785 have an objection-able feature, namely the small side lobes on either side of the main beam. Sometimes difficulties and mistakes arise in radar due to signals being transmitted and received back via the side lobes, as well as by the main lobe. Side lobes may be eliminated by Tapered Feeding which may be explained as follows :-

Take two half-wave aeri-als placed  $\lambda/2$  apart and fed equally and in phase. Neglecting the field-strength factor of the individual aeri-als, which may be introduced as a correction factor at a later stage, the field-strength diagram is as shown in Fig.782 . There are no side lobes, but the main beam is, of course, very wide. The field-strength factor obtained from (56) with  $n = 2$ , is

$$\frac{\sin \left( \frac{180^\circ \sin \theta}{90^\circ \sin \theta} \right)}{\sin \left( 90^\circ \sin \theta \right)} \dots\dots\dots (69)$$

A plot in polar co-ordinates is shown in Fig. 798. The phase centre X is half-way between the aeri-als , and they may be replaced by a source positioned at that point. Now take another similar pair of aeri-als fed with the same currents as the first, and place the two pairs together as shown in Fig.799 . Each pair is replaceable by a source at its mid-point so that the arrangement of Fig.799 is equivalent to that of Fig.780 , i.e. two sources  $\lambda/2$  apart. The field-strength diagram of these two sources is the same as the original. Hence the resultant field-strength diagram of the arrangement of Fig.799 is equivalent to that of three aeri-als fed with currents 1, 2, 1 units respectively (Fig. 801 ).



Fig.798.- Field-strength diagram of two aeri-als spaced  $\lambda/2$  apart and fed in phase.

The phase centre of these three aeri-als is at their mid-point. The resultant beaming factor is the square of that given in Fig.782, for the two aeri-als only. Continuing this process, combine 1, 2, 1 units with another 1, 2, 1 units placed so that the mid-points or phase centres are  $\lambda/2$  apart. Then the original beaming factor (69) again arises for this pair and the resultant beaming factor is the cube of the original one. This arrangement is equivalent to four aeri-als fed with currents 1, 3, 3, 1 units. The phase centre is at the mid-point.

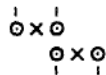


Fig. 799.- Combination of two pairs.



Fig.800.- Replacement of pairs by sources at phase centres.

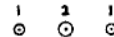


Fig.801.- Two pairs combined to form three aeri-als fed in ratio 1:2:1.

It is clear that the process can be extended and the required currents in the aeri-als will be as shown:-

<u>Number of Aeri-als</u>	<u>Currents</u>	<u>Beaming Factor</u>
2	1, 1	$T(\theta) = \frac{\sin(180^\circ \sin \theta)}{\sin(90^\circ \sin \theta)}$
3	1, 2, 1	$[T(\theta)]^2$
4	1, 3, 3, 1	$[T(\theta)]^3$
5	1, 4, 6, 4, 1	$[T(\theta)]^4$
6	1, 5, 10, 10, 5, 1	$[T(\theta)]^5$
$n + 1$	$1, n, \frac{n(n-1)}{1.2}, \frac{n(n-1)(n-2)}{1.2.3}, \dots, n, 1$	$[T(\theta)]^n$

As the original beaming factor is raised to higher powers, the beam becomes sharper. For example, consider eleven aeri-als fed with currents

1, 10, 45, 120, 210, 252, 210, 120, 45, 10, 1,

and spaced  $\lambda/2$  apart. The beaming factor of this arrangement is

$$\left[ \frac{\sin(180^\circ \sin \theta)}{\sin(90^\circ \sin \theta)} \right]^{10}$$

and the corresponding field-strength diagram is plotted in Fig.802. There are no side lobes but the beam is much wider than one would obtain with a similar number of aeri-als fed with equal amplitudes. Comparison with Figs.783,784 and785 illustrates the effect. The beam width at half

amplitude in Fig.802 is  $26^\circ$ , whereas if eleven equally fed aerials were used the beam width would be (from formula (57) or Fig.786) about  $6\frac{1}{2}^\circ$ . If the two end aerials of the present arrangement were omitted the field-strength diagram would not be altered much, since they are carrying so little current, but even then (nine elements) the beam width is much greater than that for the same number of equally fed aerials.

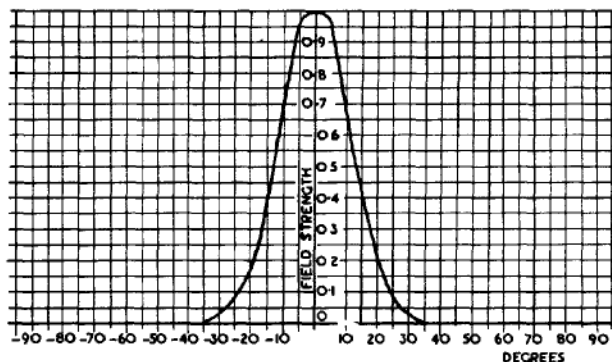


Fig.802. - Beaming factor for eleven aerials spaced  $\lambda/2$  and with binomial distribution.

The method of feeding described above involved high currents in the centre elements, tapering off to small values at the end elements. It is therefore called Tapered Feed. Since the numbers representing the currents in the elements are also the coefficients of  $x$ , in the expansion of  $(1 + x)^n$ , the distribution of currents is sometimes called a Binomial Distribution. (As  $n$  becomes increasingly large the binomial tapering tends towards the Gaussian distribution familiar in the theory of probability).

At the moment of writing this type of array is not in use, but it may be found in future developments at very short wavelengths. In any case, the principle is of importance in connection with the illumination of mirrors (see Sec. 48).

### 38. Beam Swinging with Linear Broadside Array

Instead of feeding the elements in phase as in Sec. 30 one may introduce a progressive phase difference in the radiating current elements. This may be done to any desired amount by having adjustable line-lengtheners in the feeder leads. Consider a set of radiators in a line, spaced  $\lambda/2$  apart as in Sec. 30. Suppose that each radiating element has the same amplitude but that the phase of each element lags  $90^\circ$  on the element on its immediate left-hand (Fig.803). Take rays going out from each element at an angle of  $30^\circ$  with the normal to the line of radiators. The ray from A in Fig.803 has a spatial lag of amount AC on the ray from B. Since  $AB = \lambda/2$  and CAB is a  $30^\circ$  right-angled triangle with sides in the ratio  $1:2:\sqrt{3}$ , the spatial lag AC is  $\lambda/4$ , i.e.  $90^\circ$  of phase lag. However, A is being driven  $90^\circ$  of phase in advance of B, so that on the whole these rays from A and B arrive in phase at a distant point. The main beam of the array is thus directed at an angle of  $30^\circ$  to the normal, due to this method of feeding with a progressive phase advance of  $90^\circ$ . In the case of a progressive phase difference

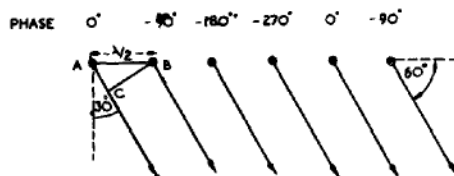


Fig.803. - Swinging of beam by progressive phase lag.

of  $\phi$  degrees between neighbouring elements the angle  $\alpha$  which the beam makes with the normal, is given by :-

$$\sin \alpha = \phi/180 \dots\dots\dots (70)$$

This applies when the centres of the elements are spaced  $\lambda/2$  apart. When the spacing is not  $\lambda/2$ , but, say,  $\lambda/x$ , then  $\alpha$  is given by

$$\sin \alpha = \frac{x\phi}{360} \dots\dots\dots (71)$$

The complete field-strength diagram is given in Fig.804 for the case of six aerials.

39. End-Fire Arrays

If the phasing of the elements of a linear array is arranged so as to swing the beam round through  $90^\circ$  from the normal, an End-Fire Array is obtained. For this to occur, with  $\lambda/2$  spacing, the phase difference between the currents in successive elements must be  $180^\circ$ . For spacing  $\lambda/x$ , the phase difference between driven elements must be equal to the phase corresponding to the spacing, so that the rays going out from the elements in a direction along the line of the array are in phase; (Fig.805)

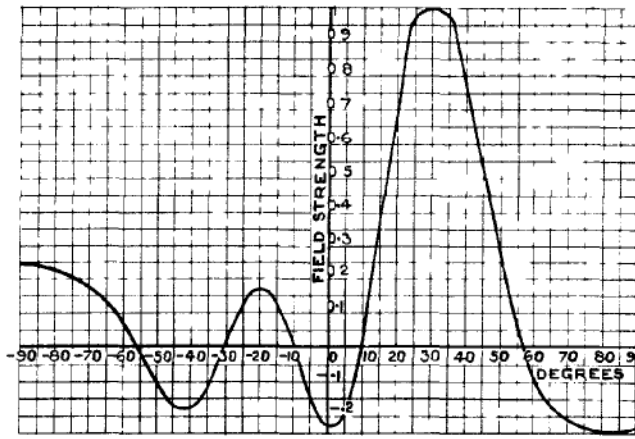


Fig.804.- Beaming factor for six aerials spaced  $\lambda/2$  apart and fed with a progressive phase change of  $90^\circ$ .

The optimum spacing of the elements is probably something less than  $\frac{3\lambda}{8}$ ; and the corresponding gain relative to a single element is about three times the length of the array expressed in wavelengths. If the elements are half-wave aerials, each of gain  $1\frac{1}{2}$ , the overall gain  $g$  relative to an isotropic radiator is

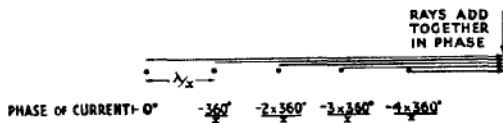


Fig.805.- End-fire array.

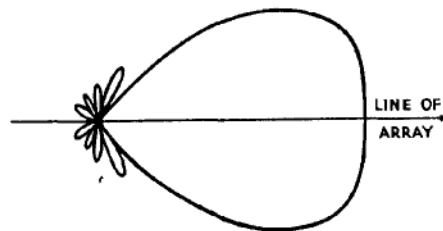


Fig.806.- Beaming of end-fire array with ten elements spaced  $\lambda/4$  apart.

$$g = 4.5 \text{ (Length of End-Fire Array in Wavelengths) } \dots\dots (72)$$

A typical field-strength diagram is shown in Fig.806. The side lobe is about 21% of the main beam. A rough rule for the beam width at half amplitude is

$$\text{Beam Width in degrees} = \frac{200 \cdot \text{wavelength}}{\text{length of array}} \dots\dots\dots (73)$$

The beaming takes place in both E- and H-planes, in contra-distinction to the linear broadside array.

40. Comparison of End-Fire and Broadside Arrays

The most notable feature of the end-fire array is the blunt end of the field-strength diagram (Fig.806) compared with that for a broadside. Consider a linear array with elements fed in phase. Rays normal to the array are in phase. As soon as one takes a direction slightly inclined to the normal, appreciable phase differences arise (Fig. 807), and the resultant field strength is diminished from the value in the normal direction. Now consider an end-fire array. The rays are in phase along the array. If one considers rays inclined at a slight angle to the line of the array (Fig.808) hardly any change in the phase difference is

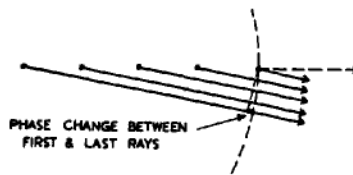
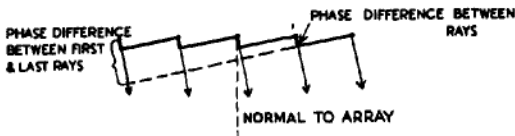


Fig.807.- Phase difference introduced by slight deviation from normal.

Fig.808.- Phase change introduced by slight deviation from line of array (phase change between successive rays is too small to show in this diagram).

introduced. The deviation from the line of the array must be quite large before these phase differences become appreciable. Hence the end-fire array produces a field-strength diagram with a blunt end. The lobe can be sharpened by making the phase of the currents in successive elements differ by an amount greater than the physical spacing of the elements. Then in the direction of the line of the array rays are already out of phase, and for the same deviation as before a greater phase change is obtained. The main beam is thus sharper, but since the maximum is not now formed by adding rays in phase, the ratio of side to main lobes is increased compared with what one would obtain from an end-fire array fed in the usual way.

41. Parasitic Director

One of the troubles of an end-fire array lies in arranging the feed of the elements in correct phase. This can be overcome to some extent by using parasitic radiators in line with a single active aerial. Consider, for example, one  $\lambda/2$  aerial connected to a transmitter and a second

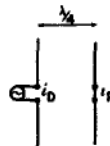


Fig.809.- Driver and parasite.

aerial, about  $\lambda/2$  long and short-circuited at its centre, placed  $\lambda/4$  away, as in Fig. 809. This second aerial is excited by the fields associated with the first, and is called a Parasite, the other being termed the Driver. Suppose the current in the driver is  $i_D$ . The field radiated from the driver is lagging  $90^\circ$  on  $i_D$  (see Sec. 4). In travelling out from the driver to the parasite the electric field suffers a further phase lag of  $90^\circ$  due to covering the distance  $\lambda/4$ . Hence the electric field at the parasite, or the EMF  $v$  induced in the parasite, is  $180^\circ$  out of phase with the driver current  $i_D$ . The parasite is regarded as a receiving aerial picking up from the driver. Owing to the fact that no load is attached to the parasite (its terminals being short circuited), all the power picked up is re-radiated. If the current at the centre of the parasite is  $i_P$  and the radiation impedance  $z_P$ , then using (29) in Sec. 14 with  $z_L = 0$ , we find

$$i_P = \frac{v}{z_P}$$

If the length of the parasite is about  $0.48 \lambda$ , its radiation resistance will be about 73 ohms and there will be no reactance in  $z_P$ . If, however, its

length is less than  $0.48 \lambda$  there will be a capacitive term in  $z_P$ ; (Fig. 810). Thus by shortening the parasite,  $i_P$  may be made to lead on  $v$ . If the

length is suitably chosen a phase lead of  $45^\circ$  may be obtained. The current in the parasite then lags on the current in the driver by  $135^\circ$  as shown in Fig. 810. This is seen to be an end-fire type of arrangement as discussed in Sec. 40. The phase of the current lags by more than the amount corresponding to the physical spacing of the elements. The field-strength diagram may be derived from first principles by considering the addition of wavelets from the driver and parasite; (Fig. 811). At a distant point along the line AB of the elements, the driver field leads the parasite field by  $45^\circ$  due to the driver's spatial lag of  $90^\circ$  ( $\lambda/4$ ) and current lead of  $135^\circ$ . However, as one moves round from the line AB the spatial lag becomes less, and thus the field at a distant point from the driver leads more and more on the field from the parasite, so that the resultant field gets less and less. At an angle of  $120^\circ$  from AB, the driver and parasite fields are anti-phase and the field is a minimum. The field-strength diagram in the H-plane is of the form shown in Fig. 812 (polar plot) with a main lobe in the line of the elements and a small back lobe. There is a minimum at  $120^\circ$  but it is not usually a zero in practice since the current in the parasite is less than the current in the driver and the two fields do not cancel.

A parasite used in this way, out shorter than resonant length, is called a director, since it helps to direct the radiation in the direction from driver to parasite.

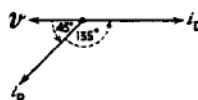


Fig.810.- Phases of currents in driver and parasite and E.M.F. in parasite when acting as a director.

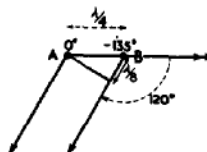


Fig.811.- Parasite acting as a director.

The length of the parasite required to provide a  $45^\circ$  phase difference between EMF and current in the parasite may be obtained from the theory of resonance applied to the aerial as a tuned circuit.

From the results given in Chap. 1 Sec. 19 ,

$$\tan \phi = 2 Q \delta$$

where  $\phi$  is the phase difference and  $\delta$  the fractional detuning; it follows that for  $\phi$  to be  $45^\circ$ ,  $2Q\delta$  must be unity. For a typical "half-wave" aerial of resonant length  $0.48 \lambda$  the ratio of diameter to wavelength is of the order of  $1/1000$ , so the  $Q$  of the resonant circuit is approximately 7 (see Sec. 12). The fractional detuning  $\delta$  must therefore be equal to  $1/4$  so that the change in length is

$$\frac{0.48 \lambda}{14} = 0.035 \lambda .$$

As mentioned in Sec. 12 the length must be shorter than that required for resonance if the impedance is to be capacitive. Hence the required length is

$$\begin{aligned} 0.48 \lambda - 0.035 \lambda \\ = 0.445 \lambda \end{aligned}$$

The current  $i_p$  then leads the EMF  $v$  by  $45^\circ$ .

Although a spacing of  $\lambda/4$  was used in the argument above, other spacings may be employed. Depending on the length of parasite and the spacing, a variety of field-strength diagrams may be obtained. Normally, it is as well to have the parasite fairly near to the driver in order to obtain a large current in it.

#### 42. End-Fire Array with Parasitic Directors (Yagi)

By using a driver and several parasites of the type described in Sec. 41 an end-fire array may be constructed; (Fig.813). Generally speaking, the phase lag of the current in any element relative to that in its left hand neighbour is greater than the phase difference corresponding to the element spacing in wavelengths. Hence this is not, strictly speaking, a simple end-fire array but is of the type described in Sec.40.

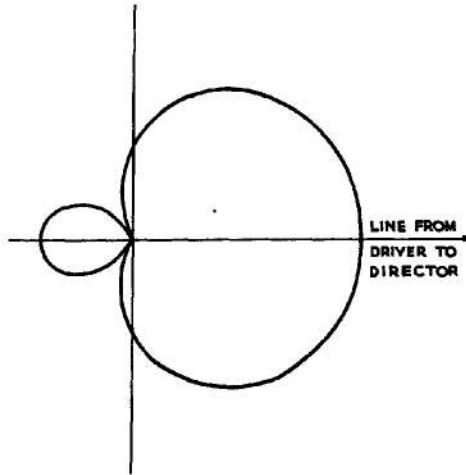


Fig.812.- Field-strength diagram of driver and director.

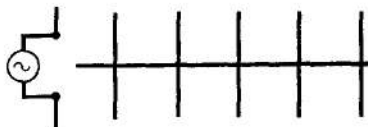


Fig.813.- Yagi aerial.

The side lobes are large and the main beam fairly sharp.

This type of array is called a Yagi Aerial. The gain  $g$  of a Yagi is probably not much different from that of a simple end-fire array, the sharpening of the beam being compensated for by the unwanted power in the side lobes. Thus using equation (62), we have, approximately,

$$g = 4\frac{1}{2} \text{ (Length of Yagi in Wavelengths) } \dots\dots\dots (74)$$

Higher gains than this are occasionally obtained by carefully varying the spacing and length of the directors, particularly with short Yagi aerials. When the Yagi is adjusted for maximum gain, the side lobes are about 30% of the amplitude of the main beam and the beam width at half maximum amplitude is roughly given by

$$\text{beam width in degrees} = \frac{130}{\text{Length of Yagi in Wavelengths}} \dots\dots (75)$$

It is emphasised that the Yagi beams in both E- and H-planes and is comparable in this effect with either a complete broadside or a linear end-fire array.

The spacing between directors is not critical and for a given spacing the director length is adjusted by trial and error to give the best result. The parasites may all be supported at their centres by an earthed metal rod (Fig. 813) since the voltage at the centre of a parasite is zero.

#### 43. Parasitic Reflector

In Sec. 41 the effect of cutting the parasite less than resonant length was discussed. It led to the result that the parasite current was lagging on the driver current. By a similar argument it can be shown that the current in a parasite in the same position as before but slightly longer than resonant length is leading on the driver current, and the maximum of the field-strength diagram is in the direction from parasite to driver. The long parasite thus appears to reflect the wave back in the direction of the driver and is called a parasitic reflector. It is also called a tuned reflector since it must be cut to a special length in order to work properly.

Parasitic reflectors are sometimes used in place of metal or netting screens behind broadside arrays; each element of the broadside has a parasitic or tuned reflector behind it. In contra-distinction to the tuned reflector a netting screen is called an aperiodic reflector.

Very often a Yagi aerial has, in addition to several directors, a reflector behind the driver. This reflector may be either a tuned parasitic reflector or a netting screen.

#### 44. Use of Folded Half-Wave Aerial

Due to the proximity of the parasites the input impedance at the centre of the driver of a Yagi is usually low, sometimes as small as 20 ohms. Transmission lines seldom have a characteristic impedance much less than 80 ohms so that a quarter-wave matching transformer or other matching device is required between driver and feeder. The use of a folded dipole enables the transformer to be dispensed with.

Take a centre-fed half-wave aerial with current  $i$  at its feed point. Extend the left arm a further half wavelength as shown in Fig.814. By analogy with transmission lines there is a current  $-i$  at the centre of the added piece and the voltages are as shown. Bend the added piece round so as to be very near the original aerial. We now have two components, each

Since the folded part is very near the driving part, the power radiated is practically the same as that for a half-wave aerial carrying current  $2i$ . Let  $R_r$  be the radiation resistance measured at the input to the folded aerial. The radiation resistance of a half-wave aerial is 73 ohms. Thus, equating powers, we have :-

$$(2i)^2 \cdot 73 = i^2 R_r$$

$$\therefore R_r = 4.73$$

$$= 292 \text{ ohms}$$

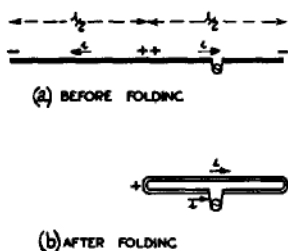


Fig.814.- Folded dipole.

In general the input impedance is quadrupled and thus a low input impedance is brought up to a suitable value for direct matching to a transmission line.

#### 45. Bandwidth of Arrays

In Sec. 40 a discussion was given of the Q-Factor of a single half-wave aerial. The calculation of the Q-factor or band-width of a large array is an extremely difficult task. The aeriels in an array are inter-coupled both by their fields and by the connecting feeder runs. Generally speaking, therefore, an array can seldom be used on any except a narrow frequency band. The following example gives an idea of the orders of magnitude; A six-element array, in use, working on 30 Mc/s. can operate at frequencies within about 500 kc/s. on either side of the design frequency. Beyond this the operational efficiency is very noticeably reduced. At high powers the maximum deviation is as low as 200 kc/s. owing to sparking and brushing which arise on the feeders when the frequency is changed. The elements of this array are constructed of thin wire ( $\lambda/\text{diameter} \approx 1500$ ). To improve the performance thicker tubing might be used, or a really thick aerial could be simulated by a wire cage type of construction. The sparking difficulty could be eliminated only by widening the feeder spacing.

#### 46. Effect of Ground on Aerial Arrays

In Sec. 24 it was shown that a single aerial placed  $h$  above ground could be replaced by two aeriels separated by  $2h$  energised anti-phase in free space, and the resultant interference pattern obtained.

Consider now an array of horizontal aeriels seen end-on in Fig. 815. Each aerial  $A_1, A_2, \dots$  can be associated with its image  $A_1', A_2', \dots$  and the image of the array is thus formed, as shown, to take account of the presence of the earth.

In the general case illustrated in Fig. 815 the free-space field-strength diagram of the aerial system is not isotropic and the method of replacing each system and its image by an isotropic radiator as explained previously cannot be used. Usually, however, any aerial systems in which ground reflections are important are set up so that the field-strength diagram of the array (neglecting the effect of ground) is symmetrical above and below the horizontal (e.g. a broadside array when used



Fig.815.- Image of array with horizontal polarisation.

in ground radar systems). In this case the field strength is the same for both direct and reflected rays at all angles of incidence and for the purpose of finding the effect of the ground the system and its image may be replaced by isotropic sources at their phase centres. The free space field-strength diagram of the system can be introduced later as a correction factor. The table in Sec. 26 applies to any array under this condition of symmetry about a horizontal plane.

47. Gap-Filling by Means of Phasing

Suppose an aerial system is split into upper and lower halves which are normally fed in phase. In order to fill the gaps in the vertical field-strength diagram, a switching arrangement is introduced in the feeders whereby the halves may be fed antiphase. Consider the aerial system AD, Fig. 816, made of two identical sub-systems AB and CD. The field-strength diagram in free space of either of the sub-systems is a graph which might, for example, be one of the graphs of Figs. 782, 783, 784 or 789. Let  $P_1$  be the corresponding beaming factor.

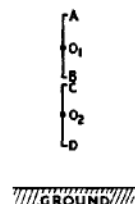


Fig. 816.- Aerial system split in halves.

Suppose the sub-systems to be fed in phase and imagine them replaced by isotropic radiators at the phase centres  $O_1, O_2$ . For the sake of argument suppose the distance between  $O_1$  and  $O_2$  is  $2\lambda$ . The field-strength diagram of the pair of isotropic radiators is shown in polar co-ordinates in Fig. 817. Let  $P_2$  be the corresponding beaming factor. The beaming factor of the aerial system AD is the product  $P_1 P_2$ . There is a main beam in a direction parallel to the earth's surface and the whole diagram is symmetrical above and below the horizontal. Reflections take place from the earth and interference lobes arise in the way explained in sections 24 to 26 and 46.

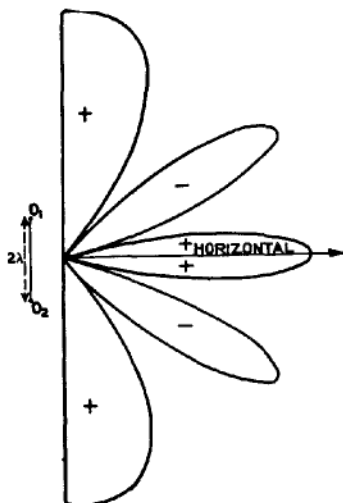


Fig. 817.- Field-strength diagram of  $O_1$  and  $O_2$  when fed in phase.

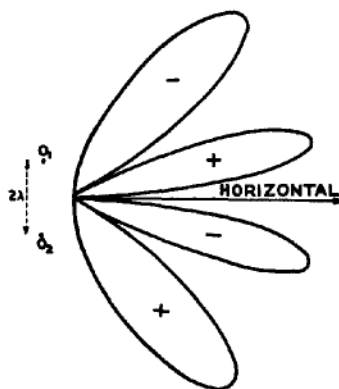


Fig. 818.- Field-strength diagram of  $O_1$  and  $O_2$  when fed in anti phase.

Next consider the sub-systems AB, CD to be fed antiphase. Replace each sub-system as before by an isotropic radiator, the two radiators this time being fed anti-phase. The resultant beaming factor is  $P'_2$ , giving the field-strength diagram shown in Fig. 818. The

beaming factor for the complete system AD ignoring the effect of ground is the product  $P_1 P_2'$ . Whatever the nature of  $P_1$  there will be no radiation in the horizontal direction since  $P_2'$  in this direction is zero. In fact the zeros of  $P_2'$  correspond to the maxima of  $P_2$  and vice versa; also the corresponding lobes above and below the horizontal are of opposite phase for  $P_2'$  and in phase for  $P_2$ . Hence where these interfere after reflection from the ground to cause zeros in one case they are additive in the other.

Thus irrespective of the nature of  $P_1$  the change in the method of feeding the two halves of the system from in-phase to anti-phase causes the gaps due to ground reflection to appear where lobes appeared before and vice versa. At the same time the main line of shoot is tilted up at an angle  $\alpha_0$  depending on the separation of the centres of the upper and lower halves of the aerial. For a separation  $\lambda$ ,  $\alpha_0 \approx 30^\circ$ ; for  $2\lambda$ ,  $\alpha_0 \approx 14\frac{1}{2}^\circ$ ; for  $3\lambda$ ,  $\alpha_0 \approx 9\frac{1}{2}^\circ$ ;  $4\lambda$ ,  $\alpha_0 \approx 7\frac{1}{4}^\circ$  and so on.

MICROWAVE AERIALS

48. Paraboloidal Mirrors

It has been emphasised in Sec. 34 that in order to attain a narrow beam and high gain, the radiating sources must be spread over as large an area A as possible. In microwave work for wavelengths of 50 cms or less, the paraboloidal mirror (Fig.819) enables the effect of distributing the sources to be attained without the use of more than one radiator. The mirror is made of metal such as aluminium alloy or copper; sometimes wire netting is employed. A section of the mirror is shown in Fig.820. The action of the mirror is similar to that which occurs in ordinary optics in the case of reflecting paraboloids.



Fig.819.- Parabolic mirror

The important point relating to a parabola is its focus F. If rays of electromagnetic radiation strike the mirror, all being parallel to the axis FO, the rays converge at F. A focal plane MFN through F and perpendicular to OF usually coincides with the aperture of the mirror. Suppose now that a radiating element is placed with its phase centre at F. Draw rays going out from F and being reflected at the surface of the mirror. After reflection the rays are all parallel to the axis OF. Further, if we consider the focal plane MFN, then all rays starting out from F reach this plane in the same time; i.e., in Fig.820 all the paths FAB, FHG, FKL are the same length. Thus, F being the phase centre of the radiator, the rays crossing the plane MFN are all in phase so that MFN is an equiphase surface. We can regard this equiphase surface as constituting a radiating area A filled with radiating sources, and the field-strength diagram, etc., can be determined from a knowledge of these sources just as in the case of a broadside array.

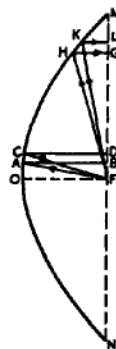


Fig.820.- Section of paraboloid.

The strengths of these effective sources distributed across the circular aperture MFN depend on the field-strength

diagram of the primary source at F. If the primary source produces a uniform distribution of field strength across the aperture then the results are comparable with what one obtains in the theory of broadside arrays. There is a main lobe with side lobes and the gain  $g$  is given by formula (58)

$$g = \frac{4\pi A}{\lambda^2} \dots\dots\dots (76)$$

The beam width at half amplitude is approximately

$$80 \lambda/d \text{ degrees} \dots\dots\dots (77)$$

where  $d$  is the diameter of the mirror in the aperture plane (cf. formula 57). The first side lobes on either side of the main beam are 13% of the maximum amplitude (compare Secs. 30 and 31 which give 21% side lobe).

Thus with the circular aperture, the beam is wider and the side lobes less than from an equal rectangular aperture, but the gain is the same.

A uniform distribution across the aperture is never obtained in practice due to the peculiar field-strength distribution which would be required from the primary source at the focus. For example, referring to Fig.820, rays FA, FC have been drawn enclosing an angle of  $5^\circ$  and resulting in the illumination of a region BD in the aperture plane. Another pair of rays FH and FK enclosing an angle of  $5^\circ$  illuminate a region GL in the aperture plane. It is clear from the figure that LG is about  $1\frac{1}{2}$  times BD. Thus, if the aperture is to be equally illuminated, less power must be sent out from the primary source at F in the direction FA (or FC) than in the direction FH (or FK). Indeed the primary source must have a distribution such that the field strength (at a given distance) in the direction towards the edge of the mirror is twice that (at the same distance) in the direction of the centre of the mirror. The power density at the edge must be four times that at the centre.

Most primary sources give less field strength towards the edge of the aperture plane than at the centre. The feed is thus tending to be tapered (cf. Sec. 37) and this results in a reduction of side lobes and broadening of the main beam in the field-strength diagram from the mirror. For a paraboloidal mirror (circular aperture) of diameter  $d$  the following data have been worked out assuming the distribution of the field strength over the aperture to be part of a Gaussian curve (see Sec. 37):

Amplitude of field at edge of Aperture divided by Amplitude at centre of Aperture	Beam Width right across between first zeros (degrees)	Beam Width right across at half max. amplitude (degrees)	Power Gain $g$	Amplitude of First Side Lobe expressed as percentage of main beam
1.00 (uniform distribution)	140 $\lambda/d$	80 $\lambda/d$	$1.00(\frac{\pi d}{\lambda})^2$	13%
0.37	162 $\lambda/d$	89 $\lambda/d$	$0.92(\frac{\pi d}{\lambda})^2$	8.5%
0.13	202 $\lambda/d$	100 $\lambda/d$	$0.76(\frac{\pi d}{\lambda})^2$	2.5%

These figures show well the broadening of beam, diminution in gain and reduction in side lobes associated with concentration of the distribution towards the centre of the aperture plane.

49. Primary Feeds for Paraboloidal Mirrors

(i) Rear Feed with Half-Wave Aerials

This is illustrated in Fig. 821. A coaxial feeder passes through the centre of the mirror and ends in a half-wave aerial with parasitic reflector. The field-strength diagram of the primary source is different in the E- and H-planes. In the E-plane more energy is concentrated towards the centre of the mirror and the beam from the mirror is broader in this than in the H-plane. Unless a balance-to-ubalance transformer is used RF currents flow on the outside of the coaxial due to one leg of the aerial being attached to this outer conductor. A quarter-wave can (skirt or bazooka) or other device is therefore attached which inserts an infinite impedance between the end of the coaxial outer conductor and the end of the can. This decouples the rest of the outer conductor from the feed point to the aerial (see Chap. 4 Sec. 38). Instead of a parasitic reflector, a small metal sheet reflector is sometimes used.

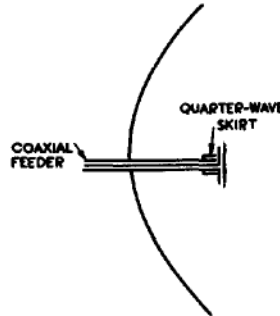
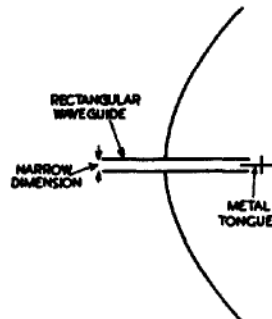


Fig.821.- Half-wave aerial with reflector for feeding parabolic mirror.

(ii) Rear Feed with Waveguide and Half-Wave Aerials

This is illustrated in Fig.822. The legs of the aerial are fixed on either side of a metal tongue projecting into the guide so that the electric field in the guide ( $H_{01}$  - mode) splits into two parts and excites the legs as it emerges from the guide.



(iii) Rear Feed with Waveguide and Slots

The guide terminates in a small cavity in which are two slots (Fig.823). These slots act as the radiating elements of the primary source.

Fig.822.- Rear feed with waveguide and half-wave aerials.

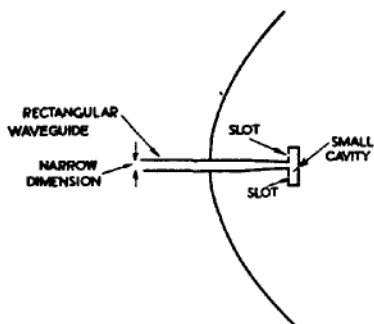


Fig.823.- Rear feed with waveguide and slots (long dimension of slots is perpendicular to the plane of the paper).

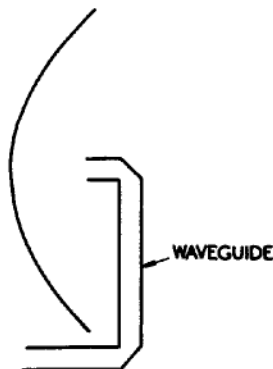


Fig.824.- Front feed with waveguide.

(iv) Front Feed with Waveguide (Fig.824)

The guide is brought round the edge of the mirror and the open end of the guide acts as the primary source. Little can be said about the field-strength distribution from the primary source at the open end of a guide. In general, the field-strength diagram is wide in a plane parallel to the narrow dimension of the guide and narrow in a plane parallel to the wide dimension.

In all the above types of primary feed, the phase centre is uncertain and must be determined by the designer in order that it may be placed at the focus of the mirror. The gains achieved in practice with these feeds are usually about 50% of the gain obtained with a uniform aperture distribution.

50. Beam Swinging with Paraboloidal Mirrors

The direction of the beam from a mirror can, of course, be altered by changing the direction of the axis of the mirror. This is not always feasible, however, and the alternative method of altering the phase distribution over the aperture is often used. If the aerial or other primary source is supported at the focus by means of an arm PF (Fig. 825), and the arm is pivoted downwards through an angle  $\theta$  to the position PF', the effect is to advance the phase of the radiation over the lower part of the aperture and to retard that over the upper part, so that the beam is tilted upwards by an angle  $\alpha$ . For small angles of tilt the relation between  $\theta$  and  $\alpha$  is approximately

$$\alpha = 0.7\theta \dots\dots\dots (78)$$

It is not desirable to tilt the beam by an angle greater than about  $\pm 5^\circ$  by this method, since the first side lobe then becomes too large.

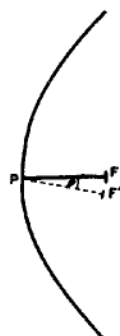


Fig.825.- Beam swinging.

51. Specially Shaped Mirrors

For some applications a narrow circular beam or pencil is not required but rather a beam which is narrow in the horizontal plane and

specially fanned out in the vertical plane. Thus, suppose a radar set in an aircraft flying at height H is required to give equal illuminations on ships at different Ranges; (Fig.826 ). Now, due to the spreading out of the spherical wavefront from the transmitter the power density falls off as  $1/R^2$  (see Sec.2). In order to compensate for this factor, therefore, one must arrange for the field distribution to be beamed more strongly in the direction of distant ships. From Fig.826 we have in triangle ABC

$$H/R = \sin \theta$$

$$\text{or } R = H/\sin \theta$$

$$= H \operatorname{cosec} \theta \dots\dots\dots (79)$$

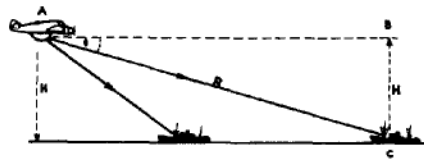


Fig.826.- Illumination of ships by aircraft.

Thus, if the power varies as  $\operatorname{cosec}^2 \theta$ , the factor  $1/R^2$  will just be compensated and uniform illumination will be obtained. Power being proportional to the square of the field strength, the field-strength diagram of the aerial in the vertical plane must be of the form of  $\operatorname{cosec} \theta$ . To obtain a  $\operatorname{cosec} \theta$  diagram the mirror must be suitably shaped. It appears that this shaping can be derived approximately from geometrical optics, i.e. assuming that the angle of incidence of each ray on the mirror is equal to the angle of reflection. From this it may be deduced that the mirror should take the form illustrated in Fig. 827.

Another method of shaping the radiation pattern in the required manner is to split the mirror in halves and move the upper section a little in front of the lower. The focus is not quite the same for each half but the difference may be neglected and a "mean focus" F assumed; (Fig. 828 ). Consider two rays FAB and FCD, making equal angles with the



Fig.827.- Shaped mirror for  $\operatorname{cosec} \theta$  beam.

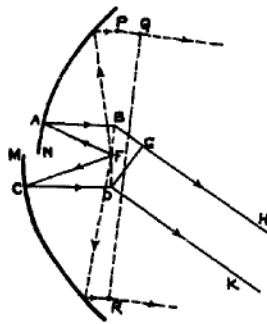


Fig.828.- Split mirror for  $\operatorname{cosec} \theta$  beam.

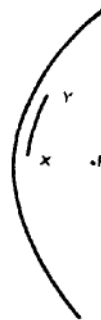


Fig.829.- Extra plate for  $\operatorname{cosec} \theta$  beam.

axis. The ray FAB arrives at B in the aperture plane before FCD arrives at D. Now the aperture plane is considered as being the seat of a number of radiating sources. The source at B is leading in phase on the source at D. Thus these sources reinforce in the direction corresponding to the rays BH, DK, making an angle with the axial direction. The path difference between the rays BH, DK, is the distance BG, and this path difference must be just equal to the path difference between FAB and FCD.

This is approximately equal to  $2MN$ , where  $MN$  is the displacement between the two halves of the mirror. The downward deflection of the beam is more pronounced for pairs of rays near the centre of the mirror than for those near the edge. For example, two dotted rays are shown in Fig.828. In order that their path difference  $PQ$  should equal  $2MN$  it is not necessary to deflect the outgoing rays very far downwards since these rays start from a very wide base line. In practice, therefore, only the centre portion is important for modifying the distribution in the required manner and, instead of the paraboloid being split, an additional metal plate  $XY$  is provided (Fig.829). This is attached by adjustable screws (not shown in the figure) and its distance from the main mirror is varied until the required distribution is achieved.

The gain of a cosec  $\theta$  mirror is only of the order of half that of the undistorted mirror giving a pencil beam. Such a mirror has a field-strength diagram with no zeros. It was originally termed "An Ideal Gapless Radar Aerial Array".

52. Cheese Type of Mirror

The cosec  $\theta$  aerial discussed in the last paragraph is elaborate and difficult to design. When it is merely desired to obtain a narrow beam in one plane (say the horizontal) and a less strictly specified wide beam in the other, the cheese reflector is probably simpler. It is illustrated in Fig.830, and consists of a metal parabolic cylinder with flat metal top and bottom plates. The aperture plane usually passes through the focus. The aim is to fill the aperture forming the mouth of the cheese with radiation and thus obtain a set of sources distributed over this area. The aperture then acts like a complete broadside array of rectangular shape and gives the appropriate field-strength diagram, narrow in the plane corresponding to the wide dimension and wide in the other plane. The primary feeding arrangements vary according to the polarisation of the wave in the guides.

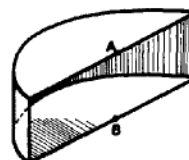


Fig.830.- Cheese reflector.

When the polarisation is such that the electric field ( $H_{01}$  - mode) is parallel to the top and bottom (or roof and floor) plates of the cheese, a flared rectangular waveguide is used. This is illustrated in Fig.831. The flaring takes place gradually in the wide dimension of the guide so that the  $H_{01}$ -mode is still present at the mouth of the flare. The width of the mouth is made  $2/3$  the height of the cheese. It is shown in Chap. 5 that the distribution of electric field in the  $H_{01}$ -mode across the wide dimension is sinusoidal in amplitude. This is shown in the full curve between the points C and D in Fig.832. The mouth of the guide is CD and the aperture of the mirror is AB, the distance between the roof and floor. The sinusoidal curve

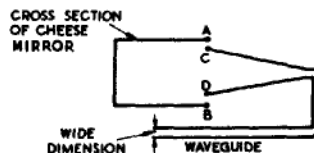


Fig.831.- Flared waveguide feed to cheese.

between C and D can be resolved approximately into two sinusoidal curves fitted into the portion AB. We may regard the cheese mirror as a type of waveguide. There are two waves present in it, the dotted curve representing the amplitude distribution for an  $H_{01}$ -wave and the dot-dash curve representing that for an  $H_{03}$ -wave. The algebraic sum of these two waves gives the original  $H_{01}$ -wave emerging from the mouth CD of the flared guide. By the known properties of waveguides, these waves travel at different speeds. The depth of the cheese and its height are so adjusted that the two waves, after reflection at the curved surface of the cheese, arrive back in the plane of the opening in opposite phase. The resultant amplitude distribution is therefore now given by the difference between the dotted and dot-dash curves as shown in Fig. 833 (full curve). It is noticeable that the field is now distributed right across the aperture, but there is an undesirable dip in the centre. However, it appears that, probably owing to the presence of higher modes, the dip is much less pronounced in practice and a reasonably uniform distribution of amplitude is obtained across the opening of the cheese mirror in the short dimension.

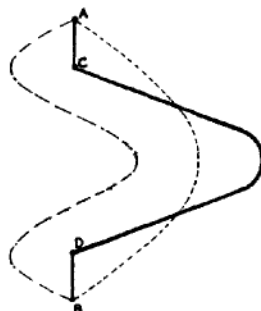


Fig.832.- Distribution of field at mouth of flared guide.

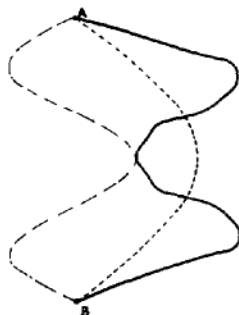


Fig.833.-Distribution of field across narrow dimension of cheese aperture.

The distribution of amplitude across the long dimension depends on the field-strength diagram of the waveguide opening in this plane. By an argument similar to that in Sec.48 it can be seen that, for uniform distribution across the opening, more power must be sent out from the guide in directions towards the edges of the cheese mirror, than towards the centre. This is unlikely to be achieved in practice, so that one can expect a tendency towards a tapered-distribution of power across the wide dimension of the aperture with corresponding diminution in gain, broadening of the beam and reduction of side lobes in comparison with the effects of uniform distribution across the aperture.

When the polarisation is such that the electric field is perpendicular to the upper and lower (or roof and floor) plates of the mirror, the method of flaring the waveguide feed does not apply. The difficulty now is to obtain a good distribution of power across the long dimension of the aperture since the waveguide is wide in this plane and directs the beam considerably into the centre of the cheese. Dielectric lenses, fastened to the waveguide mouth and designed to diverge the beam, have been used successfully.

### 53. Band-Width of Mirror-Type Aerials

In general, the frequency band over which mirror-type aerials will operate is much wider than that of broadside arrays. Consider first

the primary source, and suppose for example that this is the open end of a waveguide as in Fig.824. In the absence of the mirror, the waveguide radiation into free space but there is some reflection at the open end of the guide. If a narrow slot is cut in the wide side of the guide and a probe inserted, a standing wave will be detected. The standing wave may be eliminated by the insertion of an iris or other device near the mouth of the guide. The standing wave ratio (SWR) is then 1:1. This matching by an iris is performed at a single frequency. It is found that the frequency can deviate by nearly 10% from this value without the SWR becoming worse than 1.2:1. Similar results are found with other types of feed.

Now let the mirror be placed in position with the primary source, matched to free space, at the focus. Some of the power after scattering at the mirror comes back and is picked up by the primary feed acting as a receiving aerial. A wave thus travels down the guide or feeder and a standing wave is created due to the presence of the mirror. If the primary source is matched to free space then the SWR when the mirror is in position is given by :-

$$S = 1 + \frac{g\lambda}{2\pi a}$$

where  $g$  is the gain of the primary source and  $a$  is the focal length of the mirror. The gain of most primary sources is about 6 or 7. As a numerical example take the case of a mirror with diameter 70 cm. and consequently with focal length  $70/4$  or 17.5 cm. If the wavelength is 3 cm., then the SWR produced by the mirror is

$$1 + \frac{6.3}{2\pi \cdot 17.5}$$

$$\approx 1.2:1.$$

Smaller mirrors, with consequently smaller focal-lengths, produce a greater effect. The free-space matching is now altered so as to eliminate this standing wave. However, it is seen that the effect of the mirror is, in general, fairly small and depends linearly on the wavelength with a small factor of proportionality. The final result therefore is that a deviation of the order of several per cent can be made from the mid-frequency without undue standing waves being created on the feeder or waveguide.

The discussion above has centred round the question of the SWR on the transmission system. This is the important quantity in assessing the effect of the aerial on the transmitter valve (e.g. magnetron). Provided the SWR is not more than about 1.5:1, reasonably efficient operation is to be expected.

The alteration of the SWR due to the introduction of the primary feed into the mirror can be eliminated. This is done by placing a small raised metal plate at the apex of the mirror of such size and such position that the power scattered back to the focus is zero owing to interference effects from different parts of the mirror and plate. This gives a broader band of operation. Unfortunately this modification increases the side lobes and reduces the gain.

#### 54. Slots in Waveguides

Consider a rectangular waveguide carrying an  $H_{01}$ -wave.

Electric currents flow on the inside walls of the guide as shown in Fig.824. Essentially there are two directions of current flow, along the centre of the wide walls of the guide and transversely across the narrow walls.

The longitudinal currents may be regarded as carrying the power along the guide and the transverse currents as shunt currents which help to sustain the wave pattern but do not normally take part in the flow of power. If a thin slot AB is cut along the centre of the wide wall, the effect on the currents is negligible and power continues to flow. Similarly a thin transverse slot CD across the narrow wall does not affect the flow. On the other hand a transverse cut EF across the wide wall interrupts the currents, and radiation of power takes place from this slot. One may think of the transverse magnetic field in the wave pattern arriving opposite the slot and some of this magnetic field escaping. The magnetic field in the radiated wave is parallel to the length of the slot. Because it interrupts the longitudinal currents in the guide, the slot EF is regarded as series connected; (see also Chap. 5 Sec. 40).

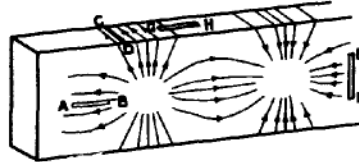


Fig.834.- Currents in walls of rectangular guide.

A longitudinal cut GH on the narrow side of the guide interrupts the shunt currents. It radiates in a manner similar to EF, being excited by the longitudinal magnetic field in the wave pattern. It is regarded as shunt-connected.

If only currents in the direction of propagation are interrupted then the slot is series connected; if only currents perpendicular to the direction of propagation are interrupted then it is shunt connected.

Slots such as EF and GH would radiate very fiercely, that is to say, they are tightly coupled to the guide and have, respectively, a high resistance and high conductance. The coupling may be weakened by altering either the position or the inclination of the slot. Positions 1, 2 and 3 in Fig.835 indicate successive loosening of the coupling for a shunt slot. Fig.836 shows the same thing for alteration in inclination.

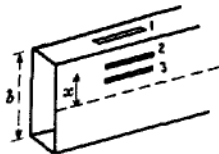


Fig.835.- Shunt slot in guide - different positions.

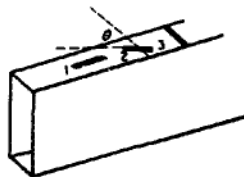


Fig.836.- Shunt slot in guide - different orientations.

Quantitative results are available for some shunt slots. Such slots are regarded as shunt elements connected across a transmission line whose characteristic impedance is taken as unity. The normalised conductance thereby obtained is then a measure of the power radiated.

In Fig.835, if  $x$  is the displacement from the centre line and  $b$  is the width of the broad side of the guide, the conductance is proportional to  $\sin^2(180^\circ x/b)$ . For a 3" guide with slot 2" long and 3/16"

wide used for wavelengths of about 10 cm., the factor of proportionality is about  $\frac{1}{2}$ , so that the maximum effect, when  $x = \frac{b}{2}$  is that of an element

of resistance 2 ohms across a line whose characteristic impedance is 1 ohm. Such a slot will radiate  $\frac{1}{3}$  of the power in a wave travelling in the guide, the remaining  $\frac{2}{3}$  passing on. In Fig.836, if  $\theta$  is the angle of rotation of the slot from the non-radiating position, the conductance is proportional to  $\sin^2\theta$ . For a guide  $\frac{1}{2}$ "x1" outside dimensions, of 18 gauge wall, with slot 0.0625" wide used for wavelengths of about 3 cm., the factor of proportionality is about  $\frac{3}{4}$ .

### 55. Slotted Linear Arrays

Based on the theory of the last section various kinds of linear arrays have been constructed with waveguides. A simple example is shown in Fig.837 with shunt slots, about a half-wavelength long, spaced half a guide-wavelength  $\lambda_g$  along the waveguide. The end of the waveguide is closed with a metal plate  $\lambda_g/4$  from the centre of the last slot. Successive slots are on opposite sides of the centre line in order to compensate for the reversal of phase in the standing wave inside the waveguide. In designing this type of array the displacement of slots from the centre line is chosen so that on the whole the guide is roughly matched, no power being reflected back. Variants of this array have the slots on the centre line and screws at the edge of each slot to distort the field inside the guide, causing the slot to radiate. Generally speaking, screws are troublesome due to their tendency to spark.

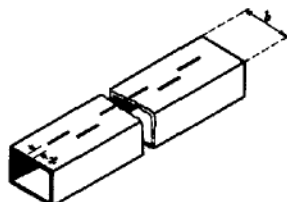


Fig.837.- Slot array with transverse polarisation.

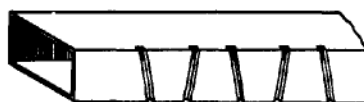


Fig.838.- Arrangements of slots in waveguides.

The type of slotted array in most favour at the moment employs cuts in the narrow side of the guide (Fig.838) inclined so as to give the required coupling. These are again shunt slots. At the same time a non-resonant design is adopted. The waveguide array as described earlier in this paragraph has a metal piston at the end and there is a substantial standing wave inside the guide. Such a system is said to be resonant and suffers from the defect that when the frequency deviates slightly from its correct value, the matching and the radiation pattern deteriorate appreciably. For a 50-element array the overall frequency bandwidth is 1% of the mid-frequency; for 200 elements it is  $\frac{1}{2}$ %. In the non-resonant design an attempt is made to produce a single travelling wave along the guide and no reflected wave. This is effected by making the centre-to-centre spacing of the slots a little different from  $\lambda/2$  (e.g.  $200^\circ$  of phase instead of  $180^\circ$ ). Then waves reflected at the slots do not reinforce one another to create a standing wave but rather tend to cancel one another out. The coupling of the slots is gradually tightened as the distance along the guide from the input end is increased in such a manner that all the slots radiate the same power. The small amount of power left in the guide after the last slot is often absorbed in a non-reflecting dummy load.

The following points are of interest regarding non-resonant arrays with slots on the narrow side :-

- (i) There is unwanted polarisation in the beam owing to the inclinations of the slots. This is said to be small in practical installations.
- (ii) The slots have to be cut carefully at the correct angle, and the fact that the angle is different for every slot introduces manufacturing difficulties. The difficulty is overcome to some extent by allowing the slots to be arranged in a succession of small groups with all the slots in a group inclined at the same angle.
- (iii) Since the slots are not being driven in phase (not being spaced at intervals of  $\lambda/2$ ) the beam is swung away from the normal to the array (see Sec. 38); in fact the beam forms part of a cone with the array as axis: this is sometimes undesirable and is eliminated by adding two triangular-shaped metal sheets (Fig. 839) which confine the waves radiated from the slots for appropriate distances so that they emerge in phase into space.

#### 56. Slotted Waveguide with Mirror

The rays emerging from the slotted waveguide array form a narrow beam radiating approximately at right angles to the array, and all the considerations of Sec. 30 and Fig. 786 apply. In the plane at right angles to the array the beam is very broad. By directing the radiation from the waveguide into a mirror (e.g. a parabolic cylinder of about the same length as the array (Fig. 840), the original beaming is retained and, due to the mirror, beaming is also introduced in the other plane.



Fig.839.- Addition of triangular plates to slotted waveguide array.

#### 57. Microwave Beacon Aerials

As remarked at the end of Sec. 30, a beacon aerial is usually required to radiate all round but with a given vertical coverage. An early type of microwave beacon aerial was the Biconical Horn (Fig. 841) excited by a small vertical aerial at its apex. Vertical linear arrays are, however, coming into use. For horizontal polarisation groups of three half-wave centred aerials are placed every half-wavelength up the length of a coaxial feeder. Probes protruding through holes in the outer of the coaxial line are used to excite the aerials (Fig. 842). The aerials stand off about quarter of a wavelength from the coaxial. Provided the point A in Fig. 842 is at a low voltage, the quarter-wave stub BAC tends to make the voltages at the points B and C oscillate antiphase. Thus the point C tends to be excited by the energy in the probe. The point D is connected to C. Thus, D and B are excited antiphase, power travels out between BA and DF and the left and right hand parts of the aerial are energised. Similar considerations apply to the other aerials. The resultant field-strength distribution is almost uniform in a horizontal plane.



Fig.840.- Waveguide array feeding parabolic cylinder.

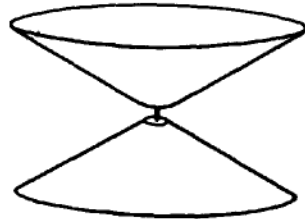


Fig.841.- Biconal horn.

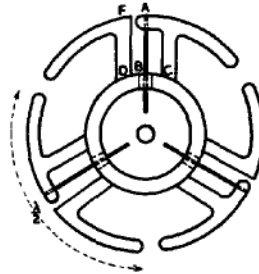


Fig.842.- Aerial array giving horizontally polarised field and a uniform field strength distribution in a horizontal plane.

58. Effect of Ground on Microwave Aerials

In Sec. 46 it was shown that the radiation from an array of aerials is affected by proximity to ground. A mirror which gives horizontally polarised waves can be replaced by an equivalent array of resonant aerials; hence its associated image can be deduced; (Fig.843). In some applications a cheese mirror (not elevatable) is used, which gives a field-strength diagram (neglecting the effect of ground) symmetrical above and below the horizontal. Let the corresponding beaming factor be denoted by  $B(\alpha)$ . Such a system can be replaced by isotropic sources at the aerial and image phase centres, and the effect of the ground deduced from the interference pattern of the two sources. For such a mirror the results of Sec.26 would hold. If the system is many wavelengths above ground there will be a large number of maxima and minima in the vertical field-strength diagram.

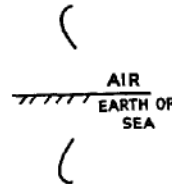


Fig.843.- Image of mirror aerial with horizontal polarisation.

59. CONCLUSION

In this chapter there has been an attempt to describe a number of types of aerial systems, and in addition to formulate the general principles of transmission and reception. Emphasis has been laid on the broadside array and its centimetre-wave counterpart, the paraboloidal mirror; also on the end-fire aerial, including the Yagi. There are, however, other aerials to be found in use with pulse systems and some of these are now mentioned briefly :-

The V-reflector aerial is one in which one uses a V-shaped instead of a parabolic reflector. The area of the aperture of the mouth of the V and the efficiency with which it is filled with radiation from the primary source are the factors determining the performance.

The polyrod or dielectric aerial is coming into use. It is an end-fire type of aerial formed by a dielectric rod along which power

travels, as in a waveguide, but at the same time a fraction of the power leaking out into space all along the surface of the rod.

The slot aerial is sometimes used as a single element. Slots in waveguides have already been discussed in Secs. 54 and 55. A single  $\lambda/2$  slot appropriately placed in the wall of any kind of cavity will act as a radiator, the plane of the magnetic field in the radiated wave being parallel to the length of the slot.

The long-wire travelling-wave aerial, sometimes used on metre wavelengths, is already familiar, being described in detail in standard works on radio.

This file was downloaded  
from the RTFM Library.  
Link: [www.scottbouch.com/rtfm](http://www.scottbouch.com/rtfm)

Please see site for usage terms,  
and more aircraft documents.

